FYS-3931

MASTER´S THESIS IN SPACE PHYSICS

Spectral observations of Polar Mesospheric Summer Echoes (PMSE)

Aquilino López Muñoz

June, 2007

Faculty of Science
Department of Physics
University of Tromsø

Acknowledgements

I would like to thank my supervisor in this work, Dr. Cesar La Hoz, for many meaningful conversations during the development of the ideas in this thesis, and for helpful comments on the text. I also want to thank him for the possibility he offered me to study a phenomenon like PMSE, which was completely unknown to me, with the difficulty that it implies for both, making available to me all the information, documents and programs that I needed.

I would like to thank the University of Tromsø for all the facilities they gave to me to carry out this project, like an office to work next to my supervisor's office or like, when ten days before my deadline, my computer broke down and they did not hesitate to lend me one during this time.

Thank to my fellow students, which always helped me in any thing I needed, specially helping me to improve my English since my arrival to Tromsø.

Finally, thanks to my family and people who love me for supporting me in all the decisions I have taken in my life.

Aquilino López Muñoz
June, 2007

Abstract

We present spectral measurements of PMSE under the influence of HF heating cycles. The data has been obtained with EISCAT VHF radar, during the EISCAT campaign 2004 in Tromsø. Examples where the PMSE overshoot appears when the electrons are heated with a specific cycle are shown. A detailed analysis of PMSE spectral width during the heating cycles concluded that there is no evidence of a possible correlation between them. In our measurements we found several frequency jumps. By analysing the abruptness one observed (with a discontinuity of the vertical velocity around 56 m/s in less than 10 seconds), we resolve for the first time how this "jump" takes place. During the transition from one Doppler velocity to the opposite, the gradual death of one Doppler velocity "layer" is observed while a new one appears increasing in amplitude until the frequency jump finishes, where the first Doppler has completely disappear and the new one has a value equivalent to the one before with opposite sign. Different models which may explain the source of the frequency jumps were tested, finding that wave steepening could explain some of the cases reported. Not many clear examples of possible signatures of gravity waves were found. In the analysis of the best candidates, we obtained values of vertical phase velocities around $c_{pz} \approx 15\text{m/s}$ and vertical wave numbers around $m_z \approx \frac{2\pi}{10}\ \text{Km}^{-1}$, which are reasonable values for atmospherical gravity waves so, we think that PMSE could be modulated by gravity waves during the EISCAT campaign.

TABLE OF CONTENTS

PROLOGUE

The thesis here presented shows theoretical studies and spectral measurements of polar mesospheric summer echoes (PMSE) under the influence of HF heating, obtained with EISCAT VHF radar during the EISCAT campaign 2004 in Tromsø.

Being involved in this project has been a big challenge mainly because of two important reasons: the little knowledge I had about this phenomenon and some of its scientific bases before my arrival to Tromsø (which explains the importance that the theoretical part had in my work) and because it was my first contact with a real investigation about one phenomenon which, in many ways, is still unknown. This last reason, like to any space physics student, was a big motivation in my work and thanks to it, I experienced sometimes great feelings thinking that maybe I was witnessing a new PMSE event for the first time.

This work is divided into two clearly distinct parts, the theoretical and the experimental. The theoretical part develops definitions, concepts and theories, making special emphasis in those that we thought more important for a better understanding of the experiments that we were going to carry out. The experimental part starts describing the work methodology that we used during the experiments and also encloses a description of the plots produced. The last part of the thesis describes the observations of the spectrograms and the analysis of the most interesting events that we found in them. This analysis is centred in 3 different types of events: events caused by the heating, frequency jumps and gravity waves. Concerning the heating, the overshoot effect described by Havnes when the electrons are heated with a specific cycle was clearly observed and several examples are shown. Also we tried to find a correlation between these heating cycles and the spectral width of PMSE but, like in previous studies, all the attempts done gave negative results. Several frequency jumps were observed in the spectrograms, the most extreme jump noticed occurs the 13th of July where a discontinuity of the vertical velocity around 56 m/s takes place in less than 10 seconds. A decrease in the spectral amplitude of one Doppler velocity “layer” while a new Doppler velocity “layer” appears increasing in amplitude with opposite sign has been observed during the frequency jumps. This is a new event that has been observed for the first time, so special attention was paid and detailed plots are shown. Also we show different models that could be the source of these frequency jumps where we conclude that frequency jumps may be a consequence of wave steepening at least in some of the cases reported. The appearance of signatures of gravity waves in our measurements is not very frequent and it is not very clear whether or not they are real signature of gravity waves. The study of two of the most evident signatures of gravity waves contribute to think that they are, since the values of some of their basic parameters (vertical phase velocities, vertical wave number and wavelength) agree with the values of atmospherical gravity waves.

A brief description of the contents of this work follows:

-The first chapter is an introduction to PMSE where we will see what this phenomenon is, some characteristics and theories that are trying to explain it.

-Chapter number 2 will deal with other phenomena connected with PMSE as the cold mesosphere or Noctilucent clouds, which are necessary to study if we want to understand PMSE.

-In chapter 3, how PMSE is measured with radars will be explained, paying special attention to EISCAT radars and to the heating facility as well as new theories developed thanks to them.

-It is known that when gravity waves reach the mesosphere, they can modulate the PMSE layers and affect other characteristics of PMSE so in the last chapter of the theoretical part, 4, a definition and the principles that govern these gravity waves will be shown.

The work done in the experimental part is divided into 3 chapters which are summarized in the next items:

-The spectral processing of PMSE data obtained during the experimental EISCAT PMSE campaign in July 2004 (Tromsø), by using existing Java and Mathematica programs with some adaptations. Chapter 5 will show the work methodology and the plots produced.

-By using the plots produced before, the explanation of the different characteristics of PMSE observed during this campaign, and the supposed location of special events like signatures of gravity waves, frequency jumps, overshoots and others not expected. This item will be covered in chapter 6.

-A detailed analysis of some of the events mentioned above and their explanations will be the aim of chapter 7.

With this thesis is attached a CD-ROM where we can observe in detail different plots produced with the data obtained with EISCAT VHF radar during the EISCAT campaign 2004(Tromsø). The CD-ROM is divided in folders which have been named depending on their contents. I also include a digital copy of the thesis in a ".pdf" file where, given that the plots have lost quality due to the pdf compression, you can observe the different plots with a higher quality than in the printed copy.

CHAPTER 1

INTRODUCTION TO POLAR MESOSPHERIC SUMMER ECHOES, PMSE

1.1 INTRODUCTION

The aim of this chapter is to get acquainted with the atmospheric phenomenon PMSE. The chapter starts with a definition of PMSE and some of its main characteristics. Also a brief history of the observation of this phenomenon will be shown. Sections 1.2, 1.3 and 1.4 cover the elements mentioned above.

Since the first observations of PMSE, several theories have tried to give an explanation for this phenomenon but none of them can explain it without doubts so it has become an interesting challenge among atmospheric scientists. The last section, 1.5 will be focused in previous theories as well as recent ones.

1.2 DEFINITION OF PMSE

PMSE→ They are strong radar echoes between 80-90 Km altitude (typically over 30 dB above the background noise in EISCAT VHF) at high latitudes in summer, normally between 50MHz and 500 MHz (VHF) and rarely at frequencies of GHz (UHF).

1.3 BRIEF HISTORY OF PMSE OBSERVATIONS

They were discovered in Alaska (1978) with the VHF 49.92 MHz Poker Flat MST radar at 65º N by Ecklund and Balsey and later Czechowsky and Rüster (1985), in Germany at 52º North found PMSE again and they assumed that these echoes were of a different nature than most of the 50 MHz echoes observed before in mid-latitudes. Since then PMSE has became a very interesting subject for researches.

The name "Polar Mesospheric Summer Echoes" comes from the fact that this phenomenon occurs during the summer period in the mesosphere, with strong echoes reaching a maximum average SNR about 30 dB while during winter they hardly reach an average SNR of 6 dB and at lower altitudes (70 -80 Km) (Rottger et al., 1988; Hoppe et al., 1988).

Nowadays during summer in the northern polar region many experiments are being carried out to study PMSE. It is known that PMSE not only appears in these locations, it can also be observed in mid-latitudes (Reid et al., 1989; Thomas et al., 1992; Latteck et al., 1999) and even at King George Island, which is located 62º S in Antartica where PMSE was observed with a received signal weaker than in the high latitudes.(Woodman et al., 1999, using 50 MHz VHF radar).

1.4 SOME CHARACTERISTICS OF PMSE

-As it is said before, the SNR of PMSE is very high compared with altitudes outside the PMSE event (typically over 30 dB for EISCAT at VHF).

-Their vertical thickness can be < 1.5 km and they appear to be horizontally stratified, though there is evidence of horizontal structure (van Eyken *et al* 1991).

-Multiple layers are sometimes seen, which are thought to be modulated by gravity waves and turbulence (Rottger *et al.,* 1988; Rottger and La Hoz, 1990).

-Typical Doppler velocity varying between -15 and 15 m/s.

-Typical spectral width around 10 m/s .

-No correlation between power, velocity and width has been clearly established so far.

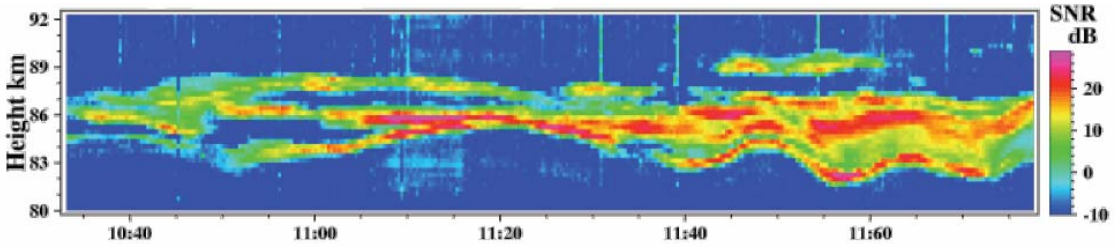

Figure 1.1→ Typical plot of PMSE Power vs Space-Time produced for the altitude region 80-92 km during the PMSE experiment, carried out on 1st July 1988 from 10:35 to 12:15 UT.

In figure 1.1 we can see some of the characteristics mentioned above:

- The red and purple colours mean SNR around 20 and 30 dB.

- In the plot, it is possible to see a multiple-layer structure where for instance, the last layer at approximately 82 km appears to be modulated by a gravity wave.

- The average thickness of these layers: about 10:50 and 11:20, there are three different layers with an average thickness of 1.5 Km, and from 11:40 until the end of the plot, PMSE becomes one thick layer with an average thickness > 4 Km.

1.5 DIFFERENTS THEORIES OF PMSE

1.5.1 Introduction

Since the first studies done of PMSE using VHF radar, the possibility of explaining PMSE with a theory of incoherent scattering was ruled out, PMSE was clearly produced by coherent scatter. (section 3.3 will talk about these two different processes). Then different theories have been proposed to explain PMSE.

These theories can be divided into two groups: turbulence theories and non-turbulence theories. Turbulence theories have as base the classical turbulence theory and non-turbulence theories started to appear due to the fact that PMSE was observed in absence of neutral air turbulence. A brief description of two turbulence and two non-turbulence theories follows in the next four sections.

1.5.2 Classical turbulence theory

This theory tried to explain PMSE by means of neutral air turbulence by assuming electrons are driven by the turbulence. But this theory failed in the attempt to explain PMSE because of the following reason:

Radar scattering is due to electron fluctuations with scales that match the Bragg scale of the radar equal to ½ the radar wavelength (chapter 3 will talk about incoherent scatter radars). Molecular diffusion in the mesosphere dissipates gradients of neutral density with scales of several 10's of meters. Thus, if the electrons that do the scattering are driven by the turbulence with the same scales as the neutrals, the molecular diffusion in the mesosphere will destroy the fluctuations.

1.5.3 Turbulence aided by enhanced Schmidt number

This theory try to correct the problem of the electron diffusion found in the classical turbulence theory.

If electron diffusion is slowed down by very massive ions, then the ratio of air viscosity (diffusion of air velocity) and the diffusion of electron can be > 1. This rate is given by the called Schmidt number Sc:

Equation 1.1

$$S_c = \frac{\upsilon_{air}}{D_e}$$

In this case where $S_c > 1$, electrons can maintain scales smaller than the neutral air scales. If S_c is sufficiently large, the electron scales could be ≤ 3 m and they will scatter the radar waves with $f_{radar} > 50$ MHz.

1.5.4 Dusty plasma scattering

Dust particles positively charged in the mesosphere will attract electrons. These dust particles have a determined velocity so the electrons will follow them with the same velocity. Under the best conditions, all the electrons will move in the same direction for a given dust particle, thus electrons will scatter in phase and coherent scatter will be produced. When this happens, the scatter power will be a function of the charge number of dust particles Z_d (La Hoz, 1992; Hagfors, 1992).

1.5.5 Dust hole scattering

If we assume the existence of neutral air vortices of several tens of meters, there is another possible explanation for PMSE in absence of neutral air turbulence. Charged dust particles of different mass would fall into one vortex. Due to the rotation movement of the vortex, the charged dust particles will be distributed around the vortex at some distance from the centre of the vortex which will depend on the mass of the dust particles. Thus large electron gradients will appear and will produce coherent scatter. (Havnes et al, 1992).

1.5.6 Conclusions

As conclusion of the theories, we could say that we still lack a theory that is able to explain this phenomenon. The turbulence theory aided by enhanced Schmidt number is the theory that may explain many properties of PMSE although it is not clear whether it can explain the existence of PMSE in the absence of neutral turbulence (La Hoz et al. 2006). In many ways, the understanding of PMSE could help to use it as a tool for the study of the coupling of different altitude regions, as a indicator for extremely low temperatures, to monitor the water content of the mesosphere, remote sensing of temperature from satellites, etc.

CHAPTER 2

DIFFERENT PHENOMENA RELATED TO PMSE

2.1 INTRODUCTION

When we start to study PMSE, one of the first things we realise is the relation between PMSE and other atmospheric phenomena, which are consequences of each other. Thus in this chapter, we will comment on some of the most important ones that are connected with PMSE.

PMSE is connected with the existence of small ice particles in the mesosphere, which exist thanks to the low temperatures in this atmospheric region during summer. Section 2.2 will explain why the lowest temperatures of the Earth occur in the mesosphere during summer.

Section 2.3 is focused in Noctilucent clouds, which is a recent phenomenon connected with the ice particles mentioned above and therefore with PMSE. This section, as in chapter 1 with PMSE, will explain what are these clouds, the first observations and some of their main characteristics.

2.2 THE COLD SUMMER IN THE MESOSPHERE

One of the main reasons for these strong radar echoes (PMSE), is the existence of ice particles with radii from a few nanometres to a few tens of nanometres, which exist thanks to the extremely cold temperature during summer in the mesosphere.

During summer, the temperatures in the mesosphere drop considerably (reaching the coldest temperatures of the Earth) but,

How and why does this phenomenon take place?

Here I show a picture that gives us an idea of the temperature variation with altitude during summer and winter.

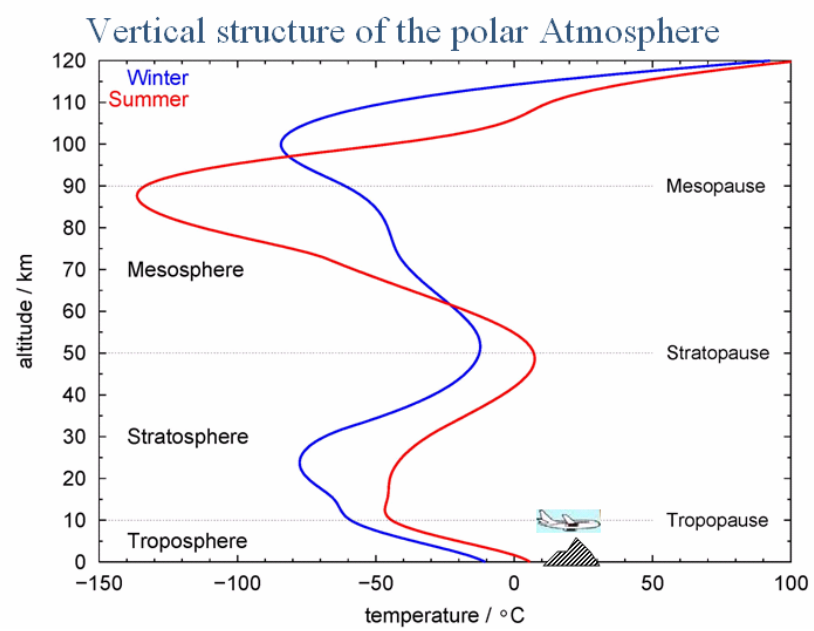

Figure 2.1→Vertical structure of the polar atmosphere.

This effect is thought to be a direct consequence of gravity waves and wind circulation around the Earth. Gravity waves can be generated due to different sources, for instance topographic generation (see chapter 4) in the lower atmosphere. These gravity waves will have an upward propagation, traveling from the dense lower atmosphere to a lighter region of it, which entails an increase of the gravity waves amplitude. The usual zonal flow in the Earth driven by the sun is easterly in summer and westerly in winter.

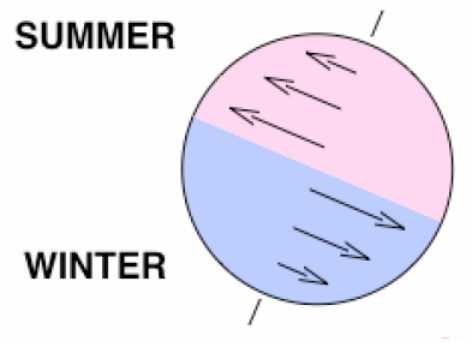

Figure 2.2→ Usual zonal flow in summer and in winter.

But this “usual flow” is broken during summer in the mesosphere. When one of the gravity waves mentioned above reaches the stratosphere in summer, a special combination of eastward and westward winds in the stratosphere acts as a filter

absorbing the zonal component of the wave more in one direction than in the other. Gravity waves continue with their upward propagation, and eventually, when they reach the mesosphere become unstable and break in the mesosphere. An analogy of this event could be an ocean wave breaking on a beach. This “wave breaking” entails an increase of momentum in one preferred direction in the mesosphere, which is able to change the summer zonal flow from easterly to westerly and also cause a meridional flow towards the winter hemisphere. The next event is flow of air travelling from the lower part of the atmosphere to the mesosphere, to keep the mass conservation. When this flow reaches the mesosphere, it will cause an adiabatic expansion and cooling. Continuing with the analogies, it is the same mechanism that refrigerators use to cool down.

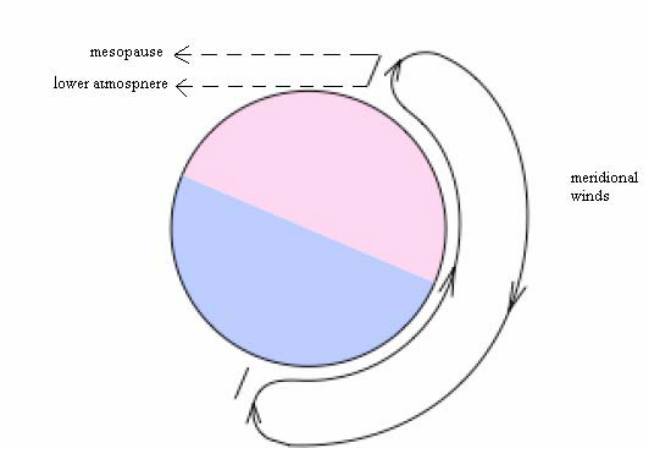

Figure 2.3→ Adiabatic expansion and cooling.

Due to these extremely low temperatures during summer in the mesosphere, we sometimes find there ice particles with radius even larger than 20 nm. And here is when we can make a relation (with a high percentage of certainly) between this phenomenon (PMSE) and another phenomenon, the noctilucent clouds (NLC) that in a way is the visible manifestation of PMSE. This phenomenon is produced by sunlight scattered by ice particles of size ≥ 50nm while PMSE are produced by radar scattering from electrons in which charged ice particles of radius < 50 nm play an important role.

2.3 NOCTILUCENT CLOUDS

2.3.1 Description

The word noctilucent comes from the Latin and it means “night shining” which gives us an idea of what they are. This phenomenon can be observed during summer nights and occurs at high latitudes. They are multi-coloured clouds, with varying intensity of blue, red and white light, the shape is close to cirrostratus clouds (both are composed of ice, but cirrostratus resides in the troposphere while NLC in the mesosphere).

Figure 2.4→ Example of NLC.

2.3.2 First observation and formation of NLC

The first NLC ever seen was in 1884, this fact indicates that it is a recent phenomenon, and this first observation coincided with the Krakatoa volcano’s eruption (1 year before), then it was believed that it could have been one of the sources that produced the NLC due to the huge amount of dust that it threw to the atmosphere, but nowadays this hypothesis is questioned because in later eruptions of other volcanoes, the observation of NLC has been normal. Then another theory about the formation of NLC is acknowledged as more reliable and tries to answer the next question:

How is it possible that there is water in the mesosphere?

It is widely believed that during the ninetieth century, with the industrial revolution and specially the increase of agriculture, big amounts of methane were released into the atmosphere, but the cause is also gas and oil fields and natural decay of

organic stuff, such as in forest. Then methane can go up and with chemical reactions becomes water in the mesosphere.

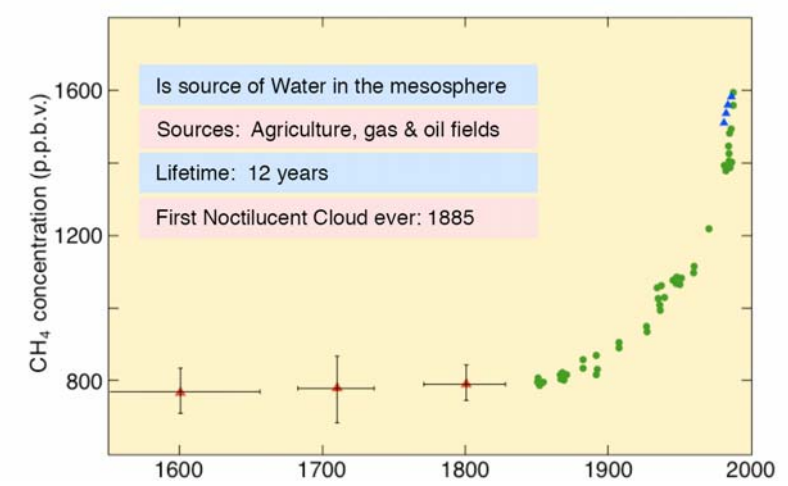

Figure 2.5→ Atmospheric methane variations.

These gases take about 12 years to arrive to the mesopause.

2.3.3 Altitudes and ranges of visibility of NLC

-These clouds are usually found in altitudes varying from 81 and 85 Km where the temperatures are around 150K (the lowest temperatures of Earth).

-In the northern hemisphere, it is possible to see NLC between mid-May and mid-August from a latitudinal zone of 50-65º N and in the south hemisphere between mid-November and mid-February in the same latitudinal zone, 50-65º S.

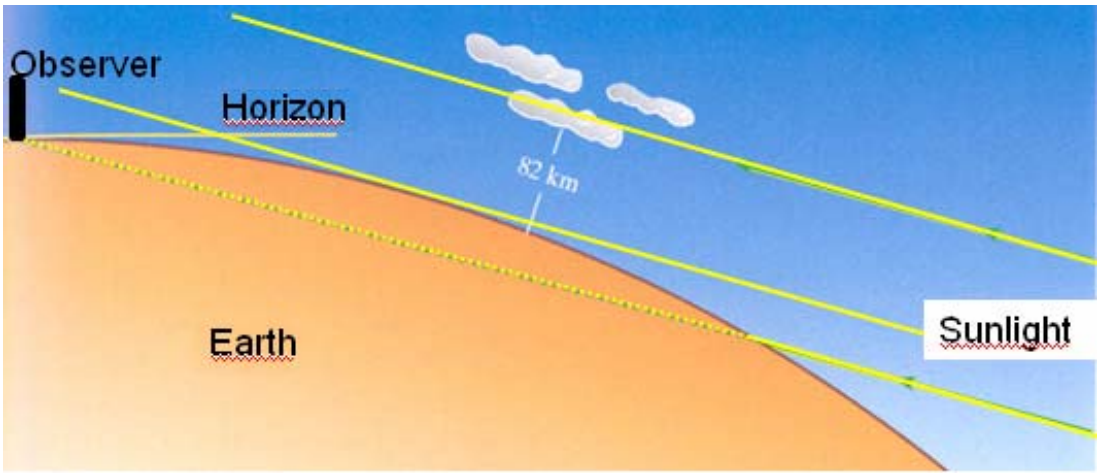

Figure 2.6 → Geometry observation of NLC.

CHAPTER 3

INCOHERENT SCATTER RADARS-EISCAT- AND THE HEATING FACILITY

3.1 INTRODUCTION

The studies of PMSE are carried out thanks to the EISCAT radars, therefore it is important to know some of their theoretical bases and the tools they use.

In this chapter, we will focus in three different parts:

- First, section 3.2 will be a brief introduction to incoherent and coherent scatter and how it is used to measure PMSE with radars. Also section 3.3 will talk about the EISCAT radars: how and in which atmospheric regions they work and where they are located.

- The second part, section 3.4, will develop the heater facility, describing what it consists of, with some technical details and effects that it causes in the mesosphere, which will be an introduction for the last part of the chapter.

- The last section, 3.5, will deal with explanations of theories and observations that have been carried with the help of the heater facility, which have been important during my experimental work.

3.2 THE INCOHERENT SCATTER MECHANISM

3.2.1 Description of the incoherent scatter mechanism

Incoherent scatter is a ground-based technique for studying the Earth's ionosphere.

With the incoherent scatter mechanism we receive in the ground-base a scattered signal caused by electron density fluctuations due to thermal fluctuations that have a wavelength equal to the Bragg wavelength, which is equal to ½ of the radar wavelength.

Equation 3.1

$$\eta_{\text{Bragg}} = \frac{\lambda_{\text{Radar}-\text{wavelenght}}}{2}$$

Since the incoherent scatter echoes received are a consequence of the thermal fluctuations of the electrons, the signals received are weak (the radars radiate effective powers around megawatts and the received signals are around picowatts).

With this incoherent echo it is possible to obtain an estimate of the ionospheric electron density. To be able to receive and process a weak incoherent scatter echo from the ionosphere, the incoherent scatter radars require the use of:

- powerful multi-mega-watt transmitters
- large high-gain antennas (typically at least 1000 m2 in area)
- sensitive receivers
- sophisticated radar control and data acquisition systems

Concentrations of different ions in the ionosphere being assumed, some of the parameters of the ionosphere and the upper atmosphere that the Incoherent Scatters Radars obtain are:

-Some basics like→ electron density, electron temperature, ion temperature, ion velocity and ion composition

-And others derived from the basics→ electric field strength, Joule and particle heating rates, conductivity and current, neutral air temperature, wind speed, fluxes of heat and plasma along the Earth's magnetic field lines.

3.2.2 Incoherent and coherent scatter

The average electron density in the mesosphere is low compared with higher regions, then using the incoherent scatter mechanism, the signal received should be lower than in these regions, but this is not what is observed, the signal received is even larger (around 3 orders of magnitude larger than it is at these altitudes). The reason is that PMSE is not produced by incoherent scatter, but is rather produced by coherent scatter.

In a coherent scatter process, the electron field of all the electrons that are causing the scatter have the same phase, while in incoherent scatter they have random phases. Here I show the consequences that these different phases have on the signal power received (which is larger with coherent scatter) with some equations:

$$\vec{E}_i \propto e^{-j\vec{\phi}_i} \qquad \text{and} \qquad \text{Power} \propto \left|\sum E_i\right|^2 \rightarrow \left|\sum_{i=1}^{n} e^{-j\phi_i}\right|^2$$

$\vec{E}_i$ = electric field of the electron "i" $\qquad$ ϕ_i = phase of the electron "i"

Coherent scatter :

In coherent scatter $\phi_1 = \phi_2 = ... = \phi_n$ being "n" the number of electrons, then:

$$\text{Power} \propto \left|\sum E_i\right|^2 \rightarrow \left|\sum_{i=1}^{n} e^{-j\vec{\phi}_i}\right|^2 = \left|ne^{-j\vec{\phi}_i}\right|^2 = n^2$$

The signal-power received in the ground-base will be a function of the number of electrons square.

Incoherent scatter :

In incoherent scatter $\phi_1 \neq \phi_2 \neq ..... \neq \phi_n$ being "n" the number of electrons, then:

$$\text{Power} \propto \left|\sum E_i\right|^2 \rightarrow \left|\sum e^{-j\vec{\phi}_i}\right|^2 = \left(\sum e^{j\vec{\phi}_i}\right)\left(\sum e^{j\vec{\phi}_i}\right)^* = \sum_i \sum_j e^{j(\vec{\phi}_i - \vec{\phi}_j)} =$$

$$\sum_{i \neq j} e^{i(\vec{\phi}_i - \vec{\phi}_j)} + \sum_{i=j}^{n} e^0 = 0 + n = n$$

Note: the summation of the unitary vectors with random phases is equal to 0 and the signal-power received will be a function of "n" (number of electrons) instead of "n^2". Thus, PMSE is due to a coherent scattering mechanism.

3.3 EISCAT RADAR

The acronym EISCAT comes from European Incoherent Scatter.

EISCAT radars use incoherent scatter mechanism with the purpose of studying phenomena in the E and F regions and in the mesosphere. They transmit very powerful electromagnetic signals. They can observe scattering from ionization irregularities created by plasma and neutral atmosphere instabilities.

The research done with these radars are varied and they are expanding the studies to different regions, for instance, the VHF radar is carrying out investigations in the mesosphere and phenomena like PMSE.

One of the most important characteristics of these radars is the large altitude they can cover: from 50 Km up to about 1000 Km, with good time resolution.

The EISCAT scientific association is in northern Scandinavia. The radars are located in Tromsø (Norway), Sodankyla (Finland), Kiruna (Sweden) and in Svalvard(Norway). The sites in Sweeden and Finland are passive receivers.

As example of EISCAT radars, it is worth to mention the two radars located in Tromsø (69º35'N, 19º13'E), one is a VHF 224 MHz radar and the other UHF 933 MHz radar. The observations that will be shown in the experimental part have been done using the data received with the VHF 224 MHz during the EISCAT campaign in Tromsø in 2004.

Figure 3.1→ Tromsø 224MHz radar.

3.4 THE HEATER FACILITY

3.4.1 Description

The heater facility is a tool that is being used with the EISCAT radars for a better understanding of the ionosphere and the neutral atmosphere that allow new experiments modifying the plasma under our control.

The radio wave from the heating transmitters has normally a frequency less than the maximum plasma frequency of the ionosphere, f_0 in region F2. The heater wave has a strong coupling, first with electrons in the D-region (partly the mesosphere) through electron-neutral collision, second with the plasma at the reflection height (normally in the F region) where there is a resonance between the wave and electrostatic Langmvir waves (this is the condition for reflection). In the first case, the result is heating of the

electrons that can be considerable (Bekele, et al 2007), and in the second case, the result is parametric plasma instabilities that cause plasma irregularities and plasma heating.

For our studies, it is the electron heating in the mesosphere caused by the heating wave that is relevant for PMSE.

A brief technical description of the heater facility follows:

- 12 linear transmitters, from 3.85 to 8 MHz all the frequencies can be tuned.

- 3 array antennas, the first has 12x12 crossed dipoles (144 antennas) with a gain of 30 dBi and 1200 MW of effective radiated power, the second and the third have 6x6 crossed dipoles (36 antennas) with a gain of 24dBi and 300 MW of effective radiated power.

In figure 3.2, we can see how they are distributed and the range of frequencies that are covered:

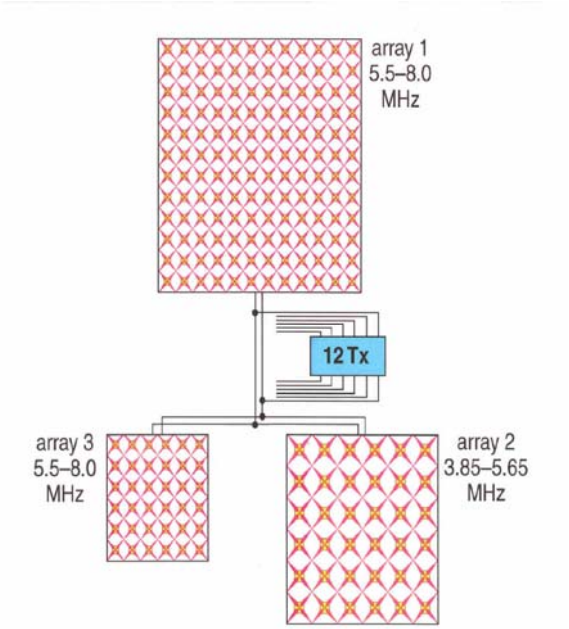

Figure 3.2→ Diagram of how the antennas are distributed and the range of frequencies that are covered

-And the control system, which is in charge of different tasks: to choose the corresponding frequency, polarization of the signal transmitted, different and complex amplitude modulations, adjust the inclination of the antennas in the north-south plane, etc.

With the heater facility, different experiments are being carried out and they can be divided into two groups, plasma physics investigations (wave-plasma turbulences and instabilities in the ionosphere) and geophysical investigations, one of these geophysical investigations is concerned by the PMSE overshoot which will be explained in the section 3.5.2.

3.4.2 How the heater facility is affecting mesosphere conditions

The way the heater facility works is also by using powerful high- frequency radiowave transmitters ≈ 5 MHz, and when these radiowaves reach the D region (PMSE is located around 84Km), electrons, are heated in a very short period of time (<1ms), due to these electrons colliding with neutrals. Depending on the electron density, the temperature will change from almost insignificant to around 3000 K. It is worth to remember that at these altitudes the temperature is the lowest of the Earth, around 150 K.

PMSE is produced by scattering from electron density fluctuations, then it is important to understand how the electron heating is affecting the echoes that we receive from PMSE and it will be shown in the next section, 3.5.

3.5 OBSERVATIONS OF PMSE USING THE HEATER FACILITY

3.5.1 First observations

In the first studies applying the heater facility to PMSE, the researchers were to find how large the influence of the electron temperature on the characteristics of the PMSE is, and how electron diffusivity is controlling PMSE.

During these experiments, they found that by heating the electrons, the power of the PMSE decreases in a very short time less than 2 seconds, (Chilson et al, [2000]) but now it is known that it is a few 10's of ms. This fast change in the electron temperature is causing changes in the electron density that becomes flatter, and one of the consequences is a strong decrease on its gradient.

It is known that PMSE is produced by scattering from electron density gradients. The fact that the echoes received are weaker while the heater is on and they recover their strength quickly after the electrons recover the environment temperature when the heater is turned off, argues that it is right.

Chilson heated PMSE in cycles with equal and short (between 10 and 20 sec) off and on periods, the PMSE power is weaker while the heater is on and recovers approximately to the same power when the heater is off.

When this cycle was used, the overshoot effect that later Havnes predicted was not known, consequently nowadays with the new campaigns using the heater facility in PMSE, it has been proved that using a cycle of 10 and 20 seconds off and on, these 20 seconds off is not enough time to return to the undisturbed plasma conditions but it can lead to an increase in the PMSE strength, the reason of this strength increase will be explained with more details with the explanation of the model that Havnes predicted of PMSE when the electrons are heated (section 3.5.2).

Some conclusions were extracted from these and later observations: an increase of the electron diffusivity due to heating is the main factor that affect PMSE and that

heating reduces the PMSE power more efficiently when the electron temperature becomes higher (E. Belova, P. Chilson, M. Rapp, and S. Kirkwood, 2001), although the first observations of the heating in PMSE was at 224MHz, it has also been observed at 933 MHz (La Hoz et al. [2003]).

3.5.2 The Havnes overshoot effect

If, instead of using this cycle of 10-20 sec switching on and off the heater, we use a different cycle where the heater is on during a short period of time and then switch it off for a long period of time (at least enough time to come back to the undisturbed conditions of the dusty plasma), we can observe the overshoot effect, which consists in an increase of the strength of the PMSE after the heater is switched off, that can be several times stronger than it was before the heater was on. (Havnes et. al 2003).

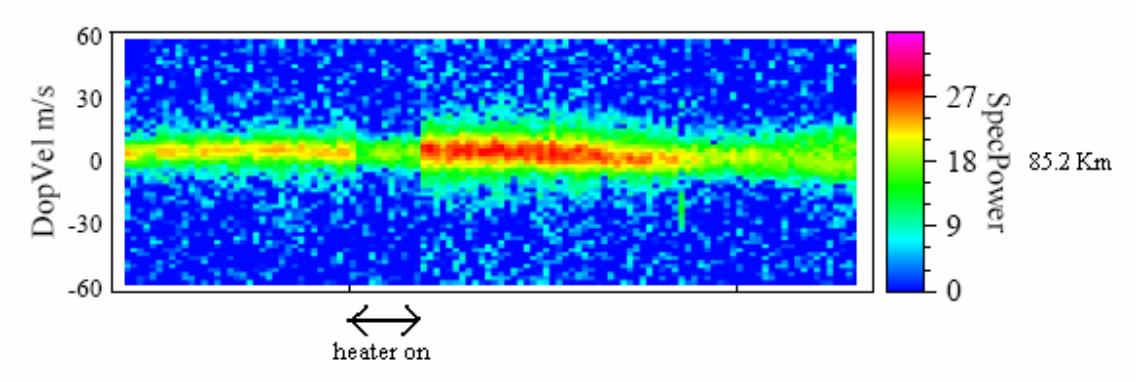

Figure 3.3→ Typical plot of PMSE Spectral Power vs DopVel-Time produced for the altitude region 85.2 km during the PMSE experiment, carried out on 5th July 2004 from 09:11 to 09:15 UT.

In figure 3.3 is observed the effect mentioned above, before the heater is turned on, PMSE SpecPower is around 21dB, during the time the heater is on it decreases 2-3 dB, when it is turned off again it increases up to 27 dB, and then it is decreasing again with the time until it comes back to the undisturbed state.

Havnes predicted what was going to happen when the electrons are heated during PMSE basing his theory on the charged ice particles.

In figure 3.4, we can see the Havnes prediction of the behaviour of PMSE power using a heater cycle of 20 seconds on and 160 seconds off, for a dust radius =50nm and ion mass =50 amu, with an increase in the electron temperature from 150º to 390º K while the heater is on:

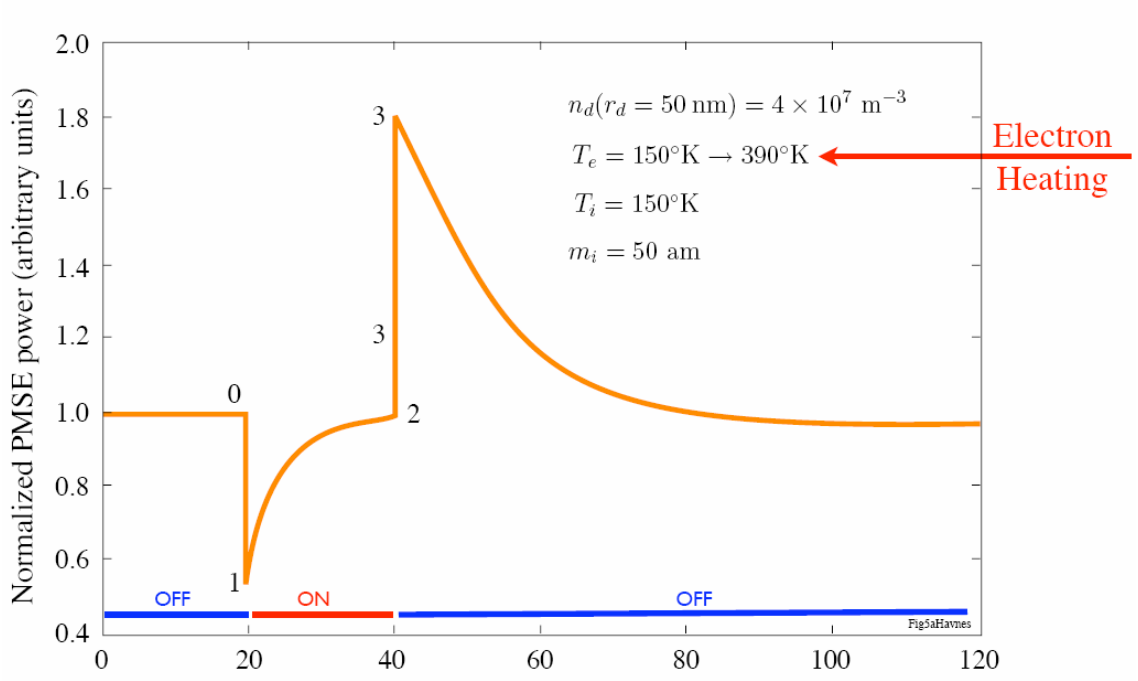

Figure 3.4→ Overshoot model, extracted from(O. Havnes,1 C. La Hoz, and L. I. Næsheim, 2003).

To explain the events observed in figure 3.4, we first have to check the Boltzmann equilibrium equation of the dust charging equations, (for a complete study of this model I recommend the lecture of "Polar Mesospheric Summer Echoes (PMSE) overshoot effect due to cycling of artificial electron heating" by Havnes, 2003, which explains other dust charging equations).

Equation 3.2

Boltzmann equilibrium: $n_\alpha = n_0 \exp(\frac{-q_\alpha V}{k_B T_\alpha})$ $\alpha = i, e$

This equation comes from the assumption than ions and electrons are in thermal equilibrium with their densities and electric field.

n_0: plasma density outside the dust k_B: Boltzmann constant=$1{,}3806503 \times 10^{-23}\,\mathrm{J/K}$

q_α = plasma particle charge T_α = plasma particle temperature

During the first 20 seconds of the figure, the heater is off and the PMSE is in undisturbed conditions (T_e=150ºK), in point "0" the heater is switched on and the electron temperature increases up to 390ºK (with Ne below 80 Km).

In equation 3.2, we can see that when the temperature of the electron decreases, the electron density profile decreases too, approaching the value to the constant value n_0, and it implies a reduction in its gradient which is observed in the figure 3.4 as a

drop in the normalized PMSE power that mainly depends on how large T_e is reduced (see figure from point 0 to 1).

After that, the heater will be on for 20 seconds. During this time, the potential V will increase (equation 3.2) to high negative value due to hotter electrons that are charging more negatively the dust. This increase of the V causes a recovery on the PMSE power (see figure from point 1 to 2).

The last step in the cycle comes now; the heater is switched off for the next 160 seconds. Just when it is switched off (point 2), the electrons come back to T_e=150ºK and a large electron gradient will appear as a consequence of the difference of potential (V in equation 3.2) and dust charges between the points 0 and 1 compared with point 2. Because of the large gradient that is produced, the PMSE strength will increase to a value larger than it was before the heater was on, in other words, appears a **PMSE overshoot** (point 3 has a larger strength than point 0). Now we only have to give enough time to PMSE dusty plasma to come back to its undisturbed state and it will be again as in point 0, for example 160 seconds .

With this brief explanation of how PMSE is affected when the electrons are heated, it is possible to presume that in the cycle using the heater 20 seconds on and 20 seconds off alternatively, in the first cycle the overshoot appeared but the next 20 seconds were not enough to come back to the undisturbed plasma condition, though the next cycle with the heater on started with a PMSE power higher than it was before the heater was on for the first time. In several cycles, the charge of the dust particles will reach a saturated value that will be constant during the alternative on off cycles.

In 2003, the first campaign to study the overshoot effect was carried out with this cycle of 20 seconds heater on and 160 seconds heater off, the predictions of the model were very successful, the measurements agreed with the values predicted. PMSE was observed at 224MHz during all the campaign and also the overshoot.

In 2004 another campaign was carried out with the same cycle of heating and a power integration time of 2 seconds. The data from this campaign has been my source of information for this work and in the experimental part (chapters 5,6 and 7) it will be shown in detail.

To conclude this section, in figure 3.5 some measurements that were taken in the campaign 2003 are compared with the predicted model. These measurements may not be as precise as we would like to study the overshoot due to several factors, as natural fluctuations on the power of PMSE and a very important one, the power integration time that was used, 5 seconds.

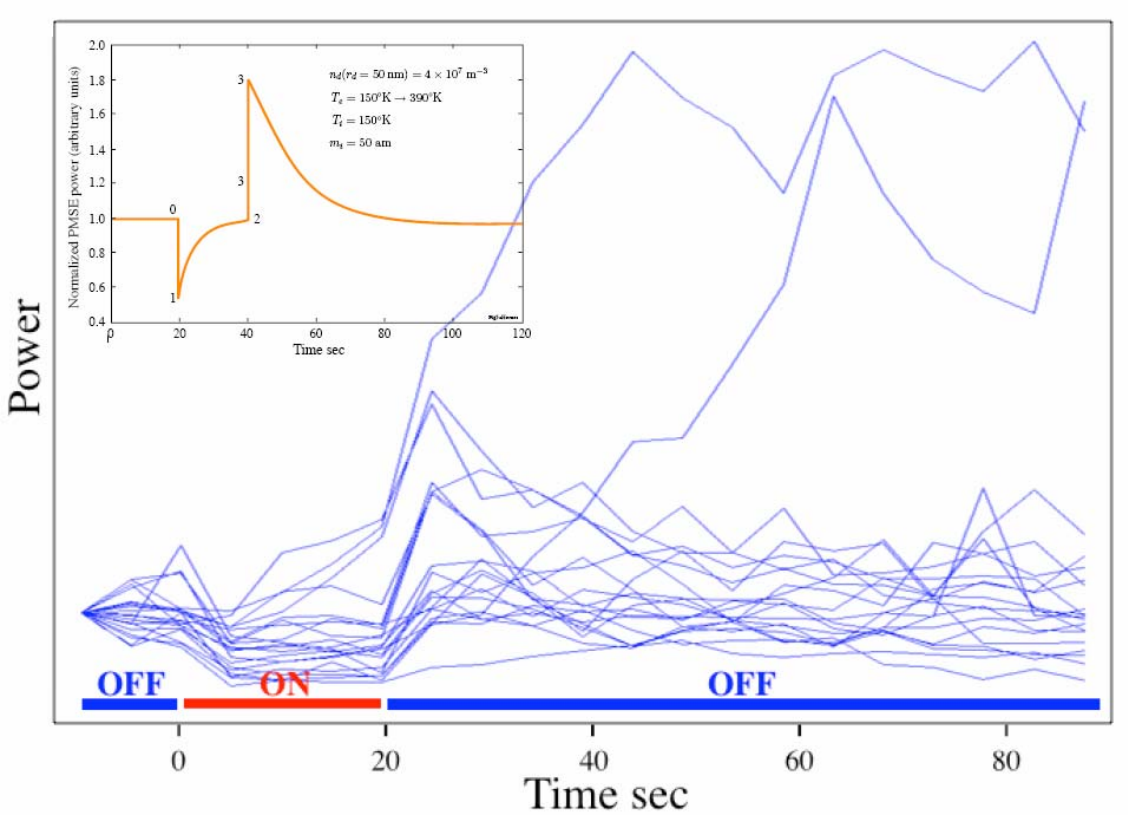

Figure 3.5→ We can see 100 seconds of each cycle , this measures where done the 2 of July-2003 from 0800 to 0900 UT .

3.5.3 Spectral width of PMSE during the heating period

In 2002, measures of PMSE were taken with the EISCAT 930 MHz UHF radar at a Bragg wavelength of 16 cm (from equation 3.1), which is not frequent (La Hoz et al, 2006). The objectives of the campaign were to search different features of PMSE and how they are affected by the HF heating.

The heater facility was working in cycles of 10 seconds on and 10 seconds off. One of the characteristics of PMSE that was studied was the spectral width of PMSE and the possibility of being affected by the HF heating. The results in this study were negative, I mean that they did not find a correlation between the PMSE spectral width and the HF heating cycles.

This negative result agrees with the idea that the HF heating is not affecting the velocity fluctuations of charged dust which determine the spectral characteristics of PMSE. A brief explanation of this concept:

The Doppler frequency is a function of the wind velocity, which may have fluctuations. The main sources of these fluctuations are: the temperature that produces random motions and in PMSE the turbulences. The heater only affects the electrons. All the ions and the neutral air are not affected by the heater.

We can conclude that when we heat, electrons become hotter with some consequences in the strength of the PMSE (sections 3.5.1 and 3.5.2) but neutral air turbulence and ions remain unaffected, then the spectral characteristics should be the same.

In chapter 7, section 7.2.3, with the new data from the EISCAT campaign on July 2004 using the EISCAT 224 MHz VHF radar, new examples will be shown with the heating cycle of 20 seconds on and 160 seconds off and we will try to find a correlation between the spectral width and this heating cycle.

CHAPTER 4

GRAVITY WAVES

4.1 INTRODUCTION

Gravity wave is an atmospherical phenomenon connected with PMSE in different ways. In the last years, the study of atmospheric gravity waves has increased, mostly in the middle atmosphere between 10 and 110 km. altitude. Between these altitudes, the density decreases significantly and the wave amplitudes increase with the altitude.

At the beginning of my work in this thesis, the study of signatures that gravity waves will impress on PMSE was the main task of my observations with the data obtained from 2004 EISCAT campaign in Tromsø, but due to the scant presence of these gravity waves along the processed data (only one or two "possible candidates" to be signatures of gravity waves on PMSE), my main work changed to the study of different effects on PMSE, like for instances, overshoot, spectral width and others, when the heater facility is used (chapter 3), which were very clear in the plots produced. But also in the experimental part, section 7.4, some observations of these possible gravity waves will be shown.

In this last chapter of the theoretical part, it will be explained what these gravity waves are (4.2), different sources that are able to unleash gravity waves (4.3) and at the end, some of the basic equations to describe these gravity waves and their vertical phase velocities, vertical wave numbers and wavelengths (4.4).

4.2 DEFINITION

Gravity waves are waves produced in a fluid medium or at the contact point between two mediums, for example the ocean or atmosphere, and that possess the gravity or buoyancy restoring force.

When a fluid parcel is displaced on an interface or internally to a region with a different density, gravity restores the parcel toward equilibrium resulting in an oscillation about the equilibrium state. This oscillation can propagate as a wave.

4.3 DIFFERENT SOURCES OF GRAVITY WAVES

Topographic generation→ Mountains have been one of the most obvious sources that are generating gravity waves interacting with winds.

Convective generation→ It is known that convection can generate gravity waves, for instance, observations of high frequency waves in the stratosphere have shown a close correspondence with deep convective clouds. This process has been the most problematic to understand mainly because it is not always observed. It is also very difficult to classify these gravity waves due to the fact that they are not characterized by a typical phase speed or frequency like, among others, topographic gravity waves, it is possible to find from high-frequency waves to low frequency waves.
Nowadays new models of these kind of gravity waves are improving our knowledge of them. These models are based on:

-pure thermal forcing
-an obstacle or transient mountain effect
-mechanical oscillator effect

Shear generation→ Since long time it is known that unstable shears can excite gravity waves. Wind shears are changes in the speed and direction of the wind between different altitudes and are associated with clear-air-turbulence, vertical flux of momentum, heat, and water vapour.

Geostrophic adjustment→During the process of geostrophic adjustment, where unbalanced fluxes change state to balanced fluxes by redistributing mean momentum, energy, potential vorticity and a radiation of excess energy away can cause gravity waves.

Wave-wave interactions→ Different characteristics of gravity waves are determined by the interaction of different non-linear waves in the middle atmosphere.

4.4 UPWARD AND DOWNWARD PHASE PROGRESSION IN GRAVITY WAVES

In chapter 7, we will try to identify signatures of gravity waves in PMSE by identifying the phase progression of the gravity waves. With that purpose, here we will see some of the equations that represent these gravity waves and characteristics.
Gravity waves can be classified depending on their phase progression, which is opposite to their propagation, it means that downwardly gravity waves have upward phase progression and upwardly propagating gravity waves have downward phase progression.

A monochromatic gravity wave with upward phase progression is defined as:

Equation 4.1

$$u'(z,t) = u_0 \cos(\omega t - mz)$$

$u'(z,t)$: horizontal wind perturbation u_0: wave amplitude at time t and height z

ω: temporal frequency m: vertical wave number

The phase of the wave is defined as:

Equation 4.2

$$\phi = \omega t - mz$$

The vertical phase velocity(time rate of change of altitude of the phase front with ϕ constant) is defined as:

Equation 4.3

$$c_{pz} = \frac{dz}{dt} = \frac{\omega}{m}$$

With the vertical phase velocity we can also calculate the wavelength of the gravity wave which is defined as:

Equation 4.4

$$\lambda = \frac{2\pi}{m}$$

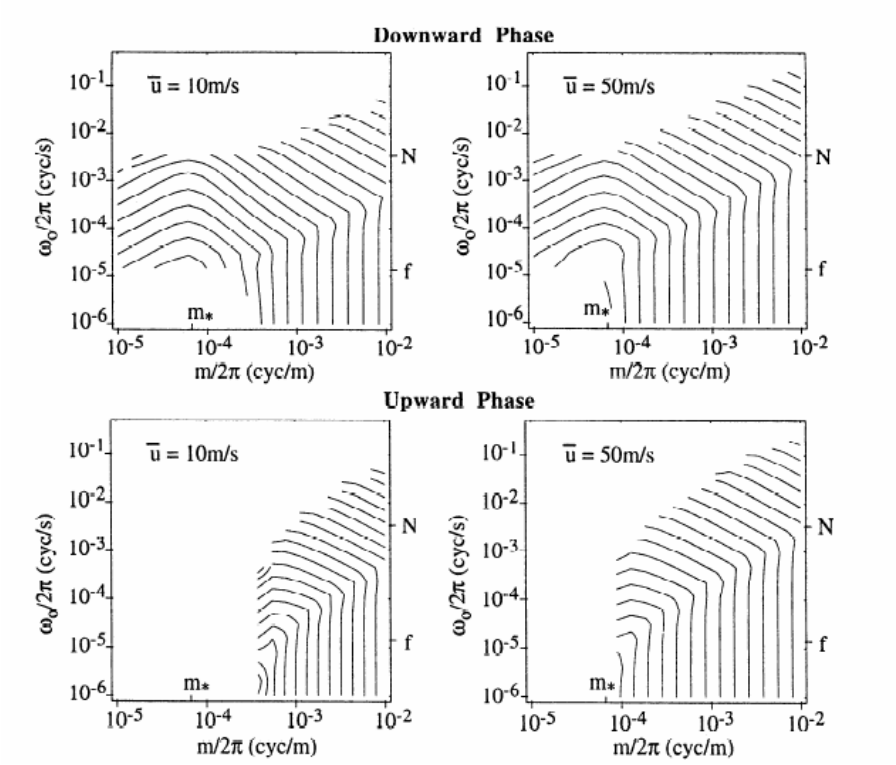

Figure 4.1→ Example of contour plots of the observed (m, ω_0) spectrum of gravity waves with downward (top) and upward (bottom) phase progression. From (Scott A. Lintelman and Chester S. Gardner,1994).

CHAPTER 5

FIRST EXPERIMENTAL CONSIDERATIONS AND DIFFERENT PLOTS OF PMSE

5.1 INTRODUCTION

-The aim of this chapter is to describe the material and methods used for the spectral processing of PMSE data, obtained during the experimental EISCAT PMSE campaign in July 2004(Tromsø).

The chapter is divided into 2 sections which will cover:

Section 5.2
- Brief description of the EISCAT campaign.
- Characteristics of the data received from the EISCAT campaign and how it is organized in order to be used.
- Electron density maps, which are a type of plots that I received already done and that I used to produce other plots with different characteristics.
- Programs used to produce the plots.

Section 5.3
- Explanation of the plots produced and which characteristics of PMSE can be measured with each one of them.

5.2 MATERIALS AND METHODS

5.2.1 EISCAT campaign

During the summer of 2004 an EISCAT PMSE campaign was carried out from the 5th until the 15th of July using the two radars located in Tromsø (69º 35' N, 19º13' S). One is VHF at 224 MHz and the other is UHF at 933 MHz (from equation 3.1, Bragg wavelength of → 67 and 16 cm respectively).

The measurements and plots that will be shown in the next chapters have been done using the received data from the VHF EISCAT radar. Here are listed some of the radar system specifications of this radar (section 3.3 to read more about these radars):

Geographical latitude	69º 35' N
Geographical longitude	19º13'E
Altitude	86.28 m
Operating frequency	224 MHz
Transmitter	2 Klystrons (vacuum tubes)
Peak power	2 x 1,5MW
Average power	2 x 150 kW
Receiver	Analogue double superheterodyne
System temperature	250-300 K
Antenna	4 of 30 x 40 m parabolic cylinders
Gain	46 dBi
Polarization	Circular

Table 5.1→ EISCAT VHF radar system specification.

5.2.2 Raw data

Raw data is the data that the real-time data-taking produces. They are composed of raw power profiles and raw correlation functions.

I used it divided in folders, which contain the data of one hour of measurements each one. In each folder, there are approximately 1800 files which correspond to one hour (the integration time that EISCAT radar used during this campaign was 2 seconds).

The different hours that comprise the whole raw data are approximately from 07:00 to 12:00 of the days from the 5^{th} to the 15^{th} of July 2004 (excluding the 9^{th} of July).

5.2.3 Ne maps (electron density maps)

As the name indicates, they are plots which show the electron density of an atmospheric region.

The Ne maps that I have used have been done with the data received for EISCAT VHF radar and between 77Km and 95 Km altitude and typically between 08:00 and 13:00 UT (both, altitude and UT, approximately).

The utility of these Ne maps in my work has been to know beforehand, and with a great accuracy, at which altitude PMSE is appearing, thus when I was processing other plots to study PMSE, I had a point of reference.

Figure 5.1 shows one of this Ne maps:

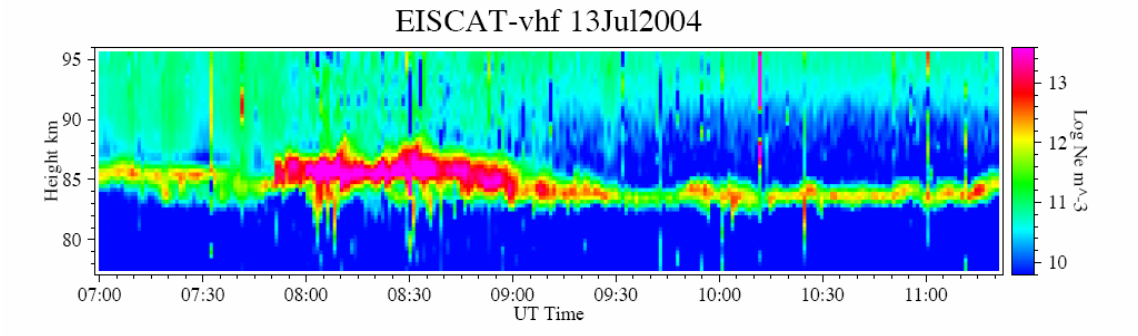

Figure 5.1→ Typical plot of PMSE Ne vs Space-Time produced for the altitude region 77-95 km during the PMSE experiment, carried out on 13th July 2004 from 07:00 to 11:30 UT.

5.2.4 Programming tools

To produce the different plots that will be shown later, I have used different programs.

- JAVA: the well known programming language orientate to objects, developed by Sun Microsystems.

- Mathematica: a very powerful global computation system developed by Wolfram Research.

-And a combination of both thanks to the product J/Link which let you call Java from Mathematica in a very easy way.

5.3 THE PLOTS PRODUCED

5.3.1 Spectrograms, Power vs Doppler velocity-time

These plots show the intensity of the echoes in a colour code as a function of Universal time and Doppler velocity for a given altitude (for a given gate).

The colour code (vertical-right axes) represents values in a logarithmic scale from 0 dB to 36 dB (rainbow colour scale with dark blue at the lowest level and magenta at the highest level), where these values have been normalized, being 0 dB the background noise in EISCAT VHF. The Doppler velocity scale, varying from -60m/s to 60 m/s, is located in the vertical-left axes.

The integration time-samples used to produce these plots was “1”, it means that the resolution that we have is 2 seconds in the horizontal axis, (remember that in the raw data each sample corresponds to 2 seconds). Each plot has been produced with 29 gates and each gate is separated from the adjacent 0.3 Km (the 29 gates cover 8.7 Km).

During my work, I have produced spectrograms (Power vs Doppler velocity-time) plots for all the hours of the raw data with all the gates where PMSE occurs with the purpose of finding features worthy of studying.

Due to the size of these plots of one hour, it is not possible to observe numeric values on a A4 paper, but in chapter 6 and chapter 7 where some PMSE features will be observed, zooms and details of these plots will be shown. Also in the CD-ROM attached to the thesis, all the plots have been included and it is possible to check them with convenient zooming.

These plots are useful to study dynamic features of PMSE as well as to study the spectral nature for each gate.

Here I listed some of the PMSE features that can be observed with these plots:

Dynamic features

-variations of the echo power
-multi-layer structure
-the overshoot effect
-PMSE layers modulated by gravity waves
….

Spectral features

-Doppler frequency jumps
-Doppler velocity variations (acceleration and deacceleration)
-Spectral width variations

And for some studies, the combination of both, as for instance, the study of spectral width variation while the heater facility is on and off.

The plots of one hour for the days 5th, 11th, 13th, 14th of July are given in the next figures as examples, and they can also be used to check some of the characteristics that I will mention later.

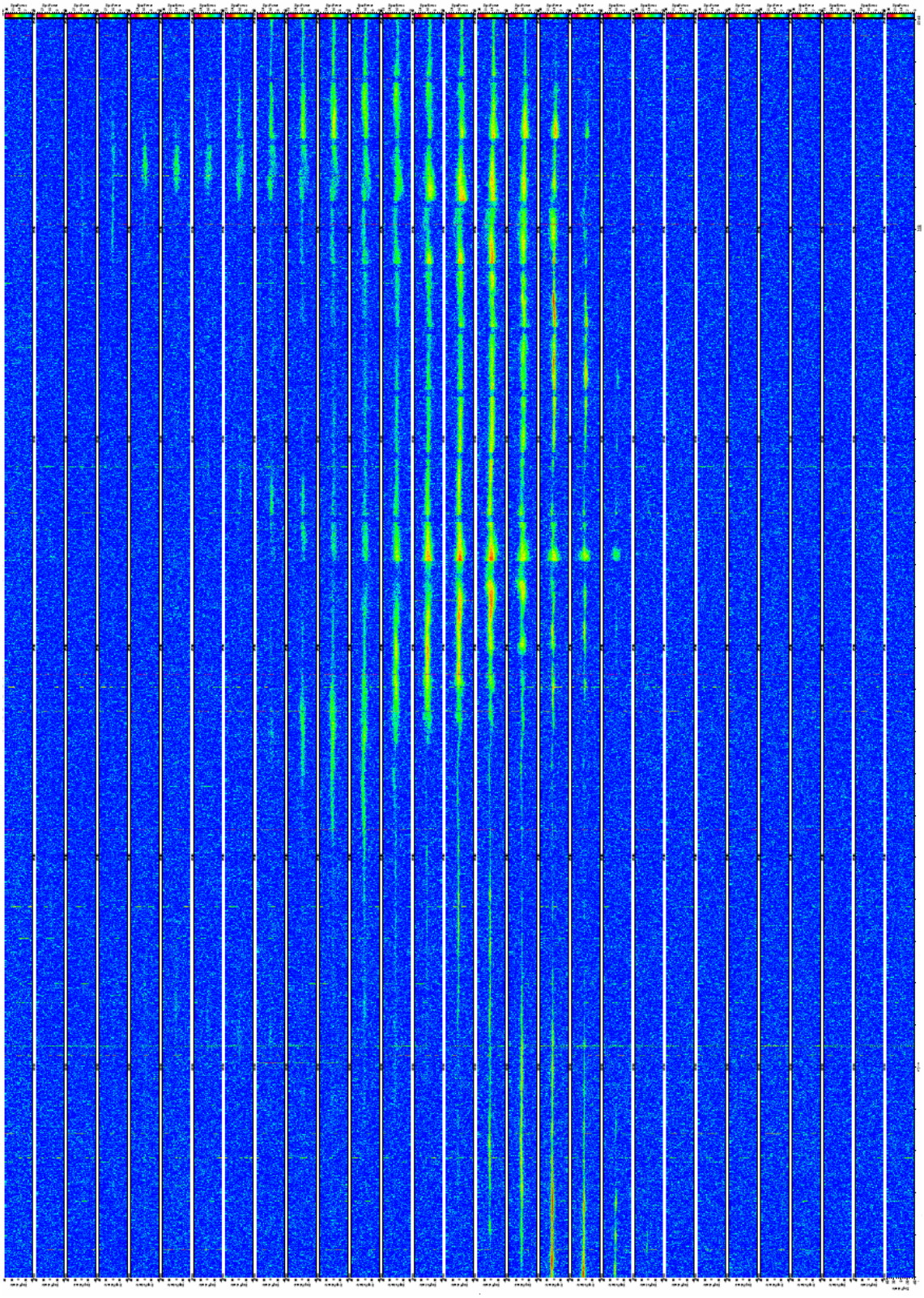

Figure 5.2→ Spectrogram produced for 29 gates, with altitudes between 81 and 89.4 km during the PMSE experiment, carried out on 5th July 2004 from 07:00 to 08:00 UT.

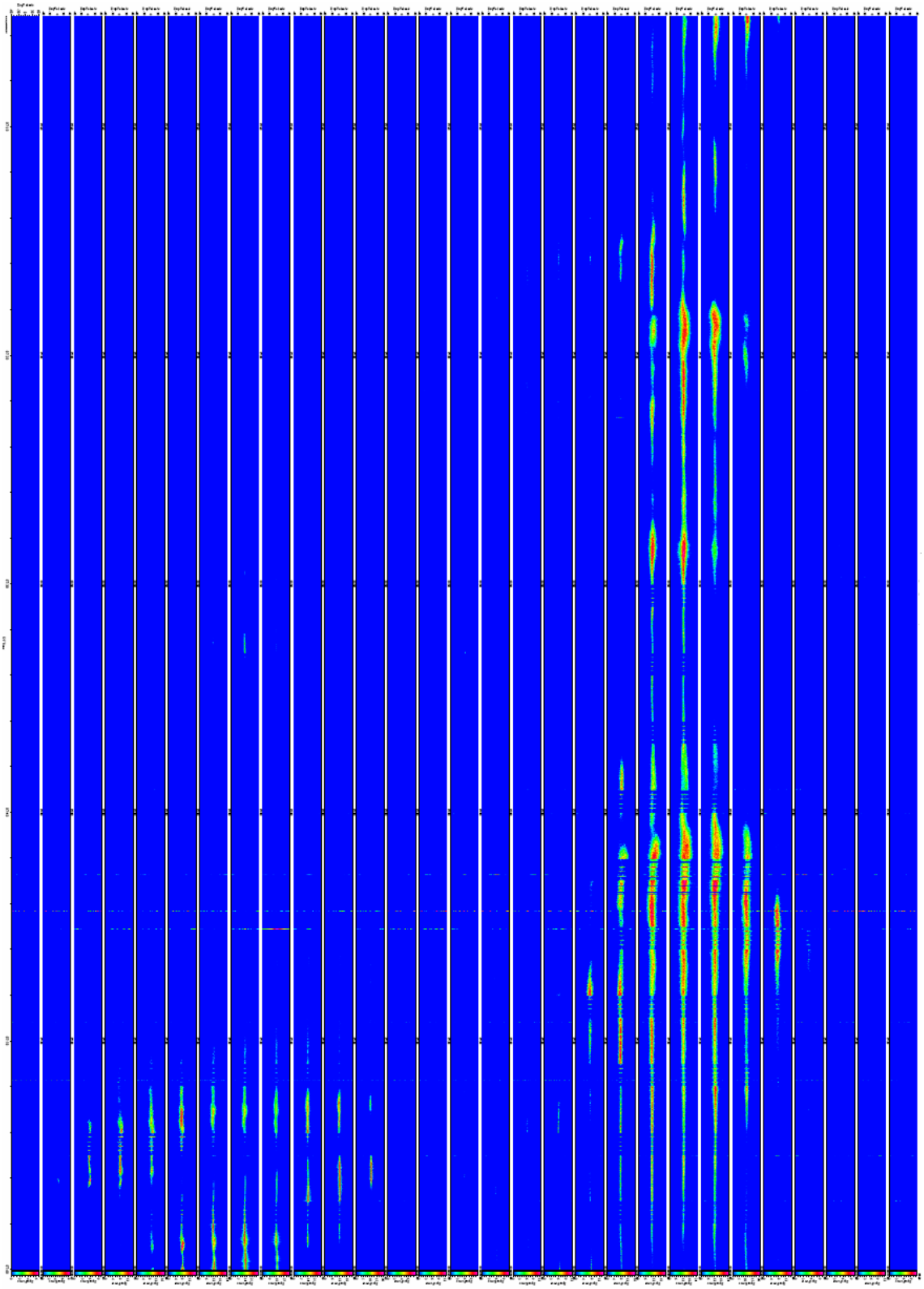

Figure 5.3→ Spectrogram produced for 29 gates, with altitudes between 79.8 and 88.2 km during the PMSE experiment, carried out on 11th July 2004 from 07:00 to 08:00 UT.

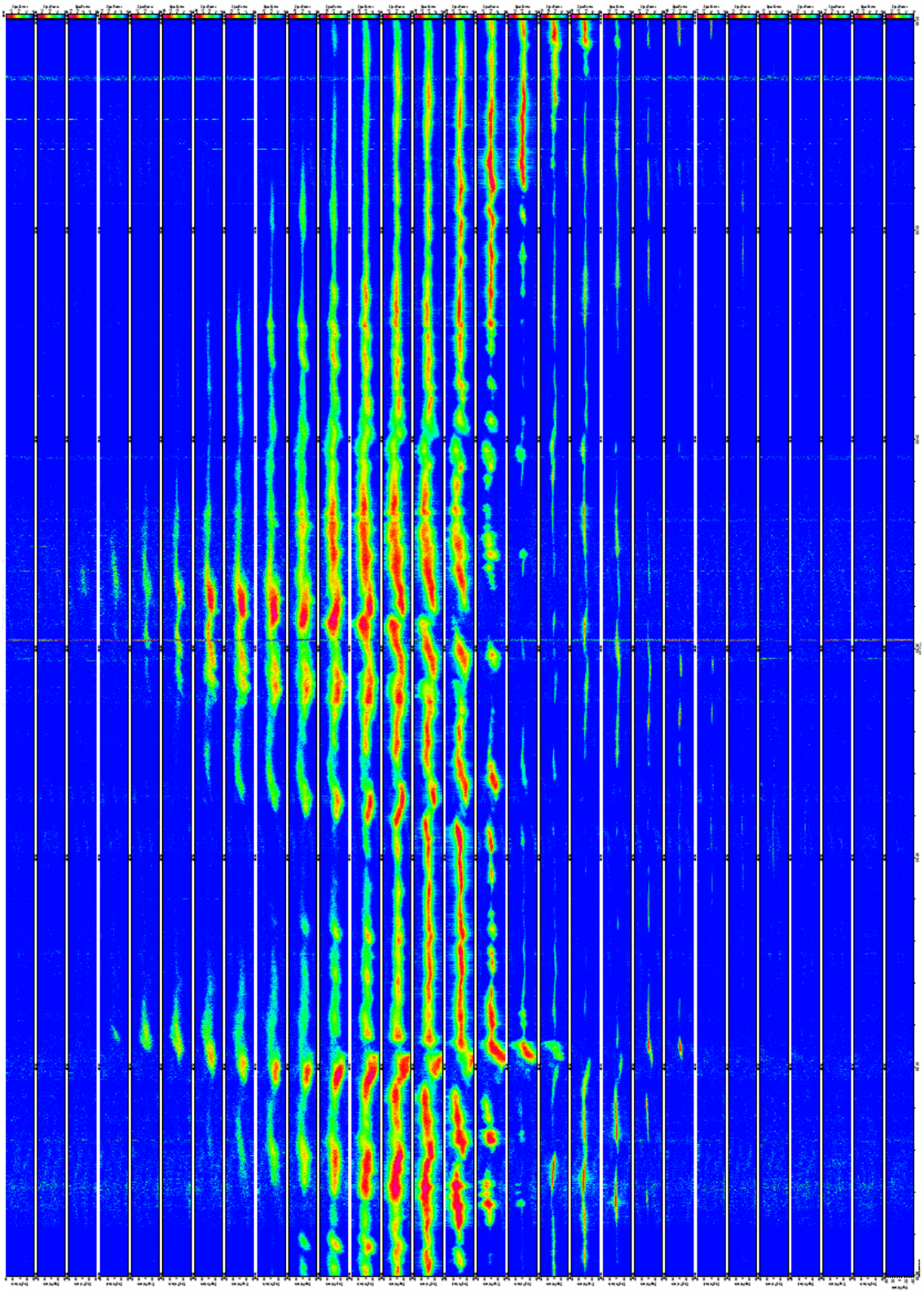

Figure 5.4→ Spectrogram produced for 29 gates, with altitudes between 81.30 and 89.70 km during the PMSE experiment, carried out on 13th July 2004 from 08:00 to 09:00 UT.

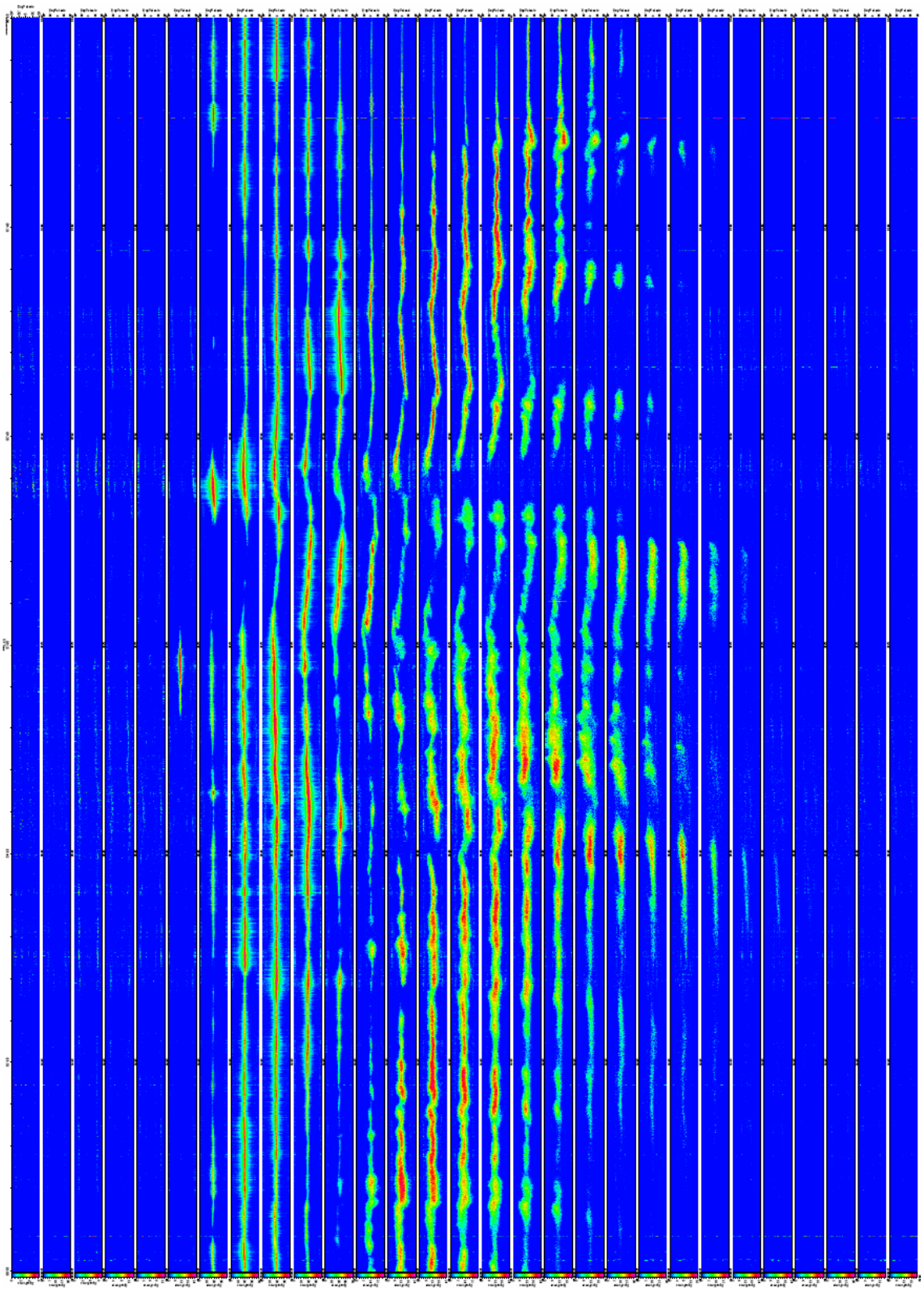

Figure 5.5→ Spectrogram produced for 29 gates, with altitudes between 80.10 and 88.5 km during the PMSE experiment, carried out on 14th July 2004 from 09:00 to 10:00 UT.

5.3.2 The spectral plots

These plots show the spectra of the PMSE signals with an integration time that can be chosen before it is produced, with a highest time resolution of 2 seconds integration time(raw data) for a given altitude(for a given gate).

The vertical axes represent the relative power, and at the same time, the plot uses a rainbow colour scale in the same way that the spectrogram Power vs Doppler velocity-time, to differentiate between different normalized-powers. The horizontal axes of each spectral panel represent the Doppler shift and it varies from 46 m/s to -46 m/s.

Depending on what was observed, I have produced different numbers of gates, each gate being separated from the adjacent 0.3 Km.
The altitudes of the gates are shown on the left side of each gate and the time is shown at the bottom of each column in Universal time.

I have mainly used two different integration-time values for these plots: 10 and 2 seconds (the maximum time resolution) depending on what I was studying.

Ten seconds to observe full hours of data and a general idea of:

-spectrum shape of one or more layers of PMSE
-width average (during the full hour)
-Doppler shift average (during the full hour)
-changes in the Doppler velocity

I have used two seconds to observe with a good resolution:

-frequency jumps (section 7.3)
-the effect of the heater facility on PMSE with two different heating cycles →overshoot effect (sections 7.2.1 and 7.2.2) and spectral width (section 7.2.3)

The next figures show two examples of spectral plots, one with 10 seconds integration time and the other with 2 seconds integration time.

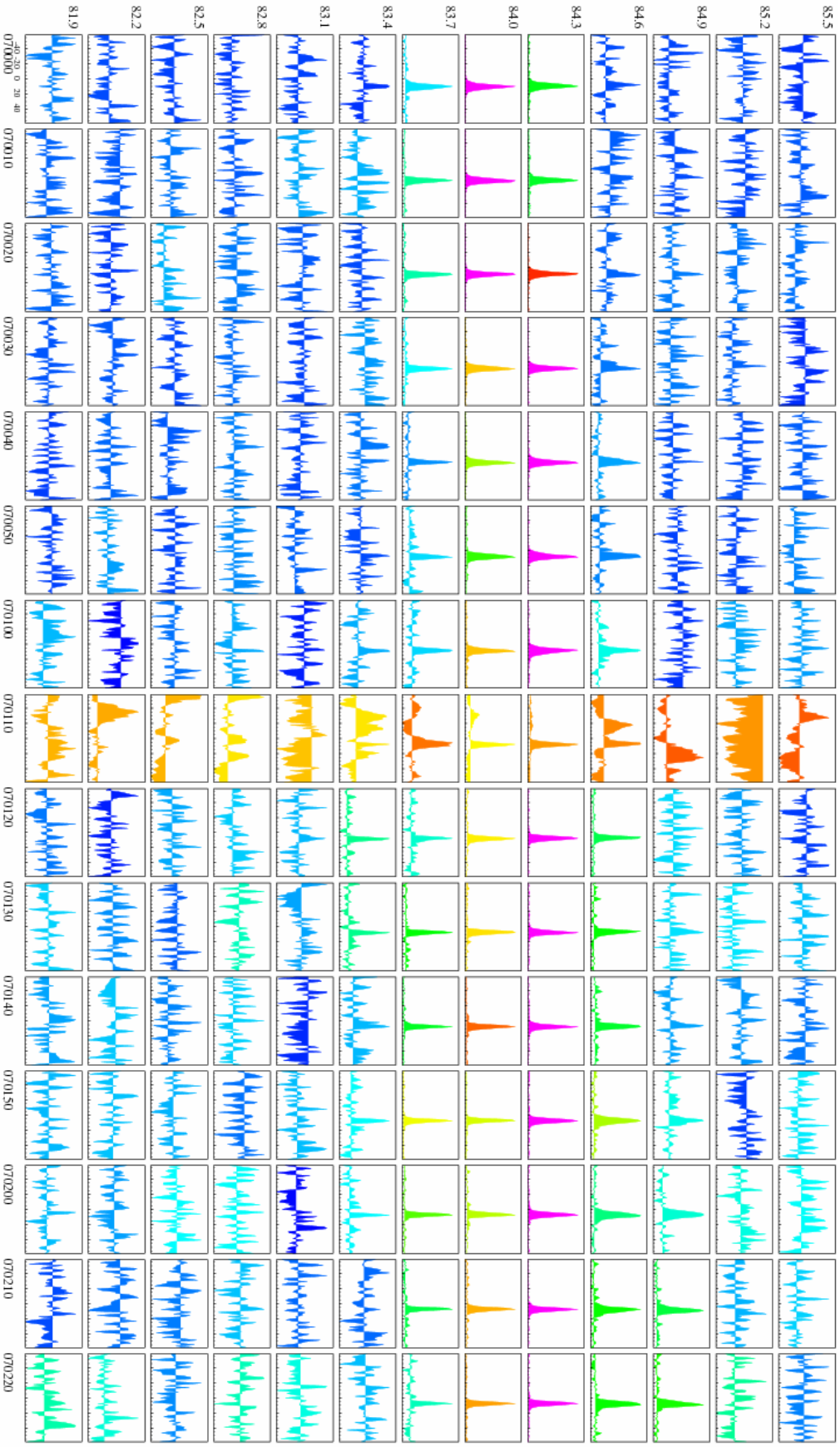

Figure 5.6→Example of PMSE spectral plot with 13 gates from 81.9 to 85.5 Km altitude and an integration time of 10 seconds, during the PMSE experiment, carried out on 5th July 2004 from 07:00:00 to 07:02:20 UT .

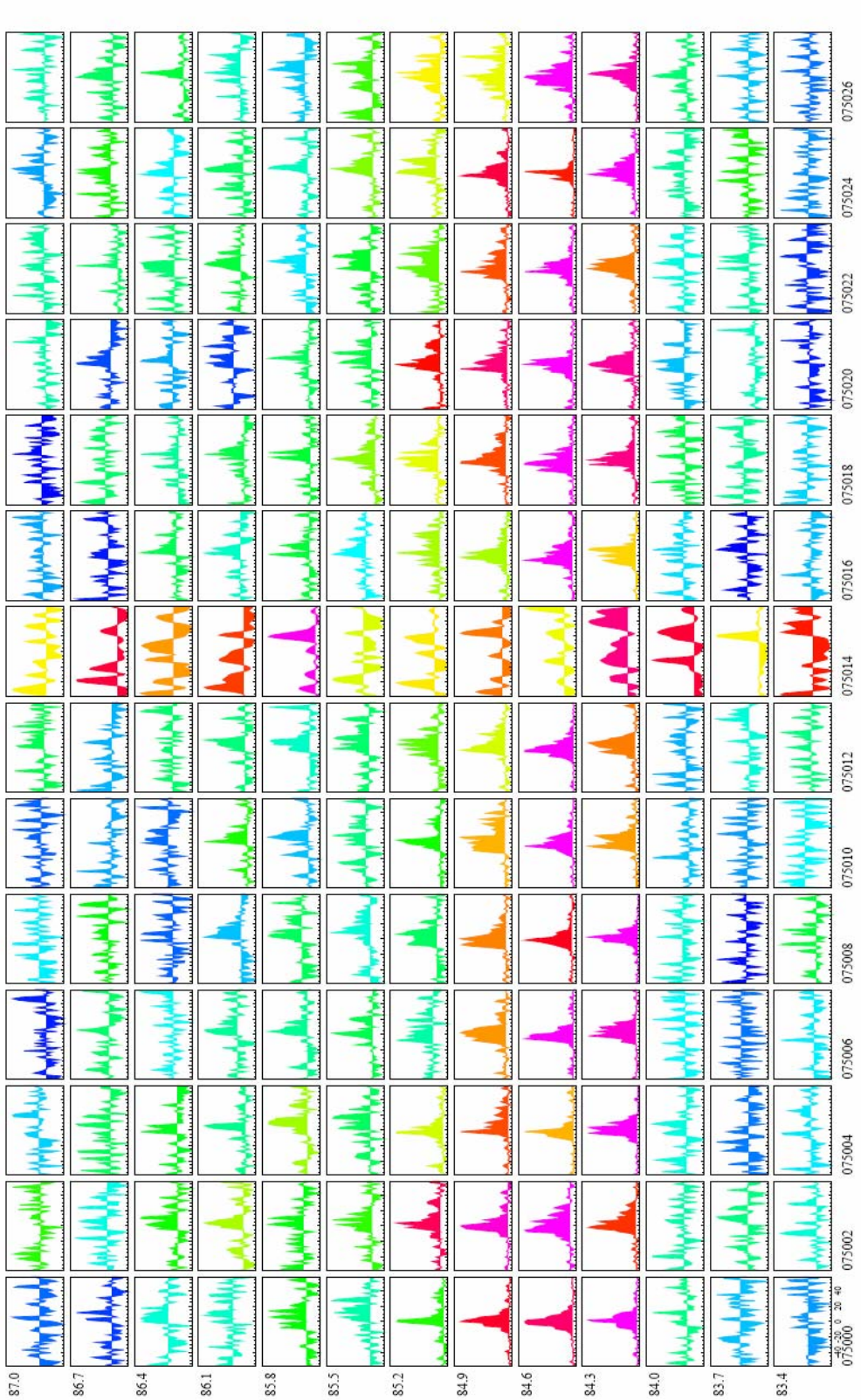

Figure 5.7→Example of PMSE spectral plot with 13 gates from 83.4 to 87 Km altitude and an integration time of 2 seconds, during the PMSE experiment, carried out on 5th July 2004 from 07:50:00 to 07:50:26 UT.

5.3.3 Plots produced by using Mathematica program

The plots produced with Mathematica have been done to study, in a very precise way, some features of PMSE that were observed before with the other plots but with less precision. Mainly these three: spectral amplitude, Doppler shift and spectral width of PMSE.

To do that, it was first necessary to do a Power-statistics study of the PMSE background noise.

5.3.3.1 Power-statistics study

This study was done for the ten days of the EISCAT campaign and here is a brief description of what it consisted of:

-To take a few noisy gates above the gates where PMSE appears.

-To eliminate the outlayers, received scattered power values which are very far from the range where they should appear, and which will cause wrong calculations on the statistics.

Figure 5.8 and figure 5.9 show the difference of the data with and without outlayers and how, eliminating a not meaningless number of samples, all the others are concentrated around the same power values.

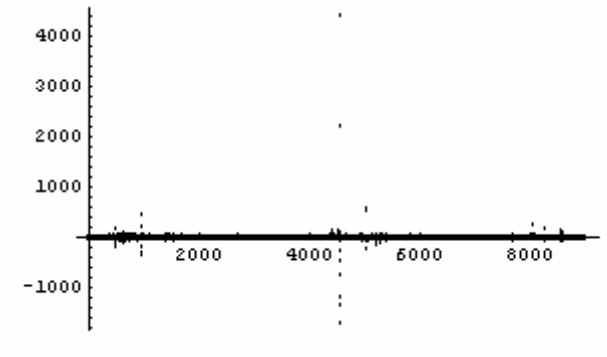

Figure 5.8→Power vs samples plot with outlayers. 13 of July 2004 from 07:59:58 to 09:00:00 and between 89.4 and 90.6 km altitude. 5 noise gates (9000 samples).

Figure 5.9→ Power vs samples plot without outlayers. 13 of July 2004 from 07:59:58 to 09:00:00 and between 89.4 and 90.6 km altitude. 5 noise gates (8950 samples).

-With these new values without outlayers, to calculate the statistics for these gates.

-To repeat the process with other gates, taken from below the gates where PMSE is appearing.

-To combine both to obtain the best values of background noise statistics (variance, standard deviation, sample range…) which will be necessary to produce other plots of PMSE spectral amplitude, Doppler shift and spectral width.

5.3.3.2 Examples of plots

In this section, some of the most important types of plots produced with Mathematica will be shown.

As in section 5.3.2, spectral plots were produced but with some differences, the spectral width, Doppler velocity and spectral amplitude were calculated by fitting Gaussian functions to the spectra.

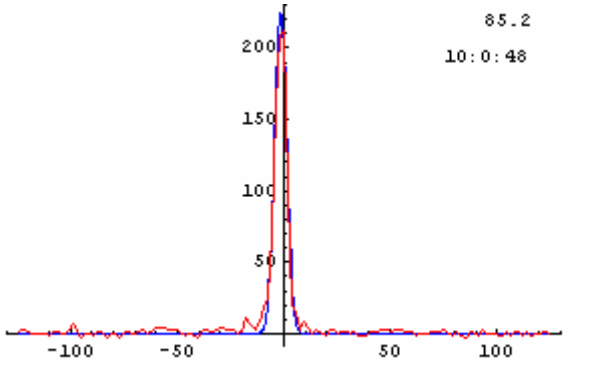

Figure 5.10→ Spectra (red) and its fitted Gaussian function (blue). The numbers on the upper right corner show the altitude in Km and the Universal time. The vertical axes shows the spectral amplitude in arbitrary units and the horizontal axes shows Doppler velocity in m/s.

With these plots, it is possible to study the same PMSE characteristics than with the spectral plots of section 5.3.2 but with the advantage of knowing their values.

Another important plot to study the spectral width of PMSE during the heating period (theory in section 3.5.3) is:

- PMSE spectral width variations of a gate for a given period of time

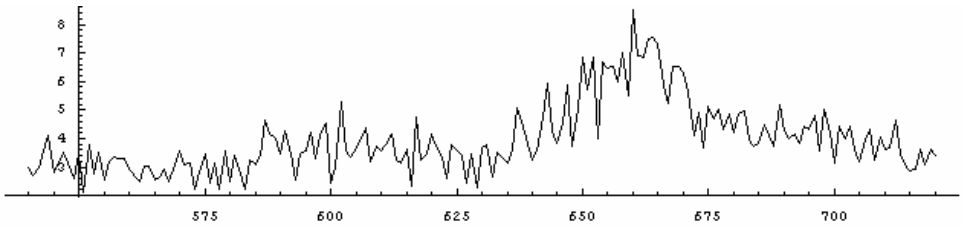

Figure 5.11→Example of random Spectral width of one gates during 6 minutes, the vertical axes is spectral width in m/s, the horizontal axes is samples(from the raw data, each sample is 2 seconds).

And combining more than one gate, to study PMSE characteristics in different layers, as for instance:

PMSE spectral width variations of "n" gates for a given period of time → in these plots, it is easy to observe at what time the spectral width in the different layers of PMSE changes.

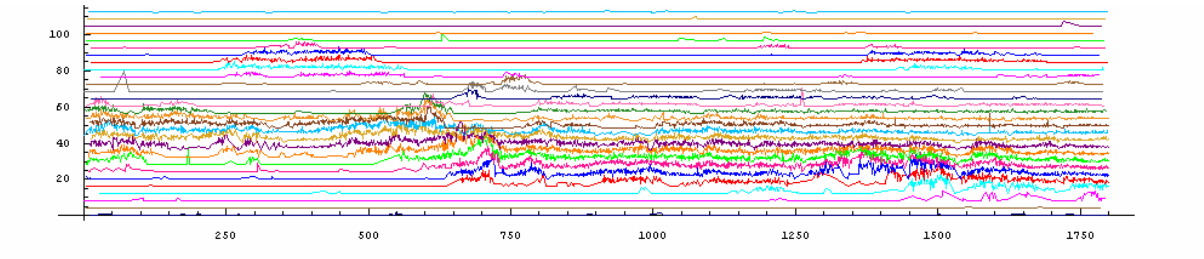

Figure 5.12→ Spectral width of 29 gates during one hour, the vertical axes is spectral width in m/s, the horizontal axes is samples (from the raw data, each one is 2 seconds). PMSE experiment, carried out on 5th July 2004 from 08:00:00 to 09:00:00 UT and from 82.8 to 91.2 Km altitude.

To study Doppler velocity and power variations, the next plots have been produced:

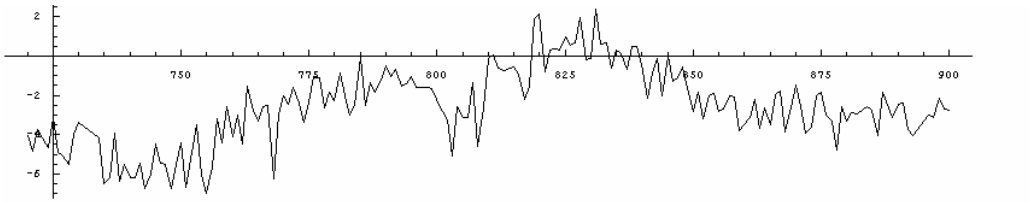

Figure 5.13→Example of random Doppler velocity of one gates during 6 minutes, the vertical axes is Doppler velocity in m/s, the horizontal axes is samples (from the raw data, each sample is 2 seconds).

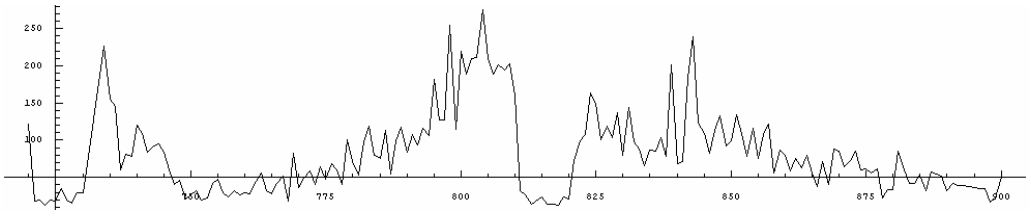

Figure 5.14→Example of random PMSE total signal power of one gates during 6 minutes, the vertical axes is PMSE total signal power in arbitrary units, the horizontal axes is samples(from the raw data, each sample is 2 seconds).

Figures 5.11, 5.12, 5.13 and 5.14 can be also plotted with time (UT) in the horizontal axes instead of samples, depending on what we need to study.

CHAPTER 6

GENERAL OBSERVATIONS OF PMSE SPECTROGRAMS DURING THE EISCAT CAMPAIGN

6.1 INTRODUCTION

The aim of this chapter is to show the different observations of PMSE spectrograms for all the days of the EISCAT campaign, with special emphasis in the events that I found more interesting to analyse. Some details will be shown of these events, and in chapter 7 they will be discussed.

It is important to mention that the heater facility was working during all the experiments all the time, with a cycle of 20 seconds on and 160 seconds off except the 11th of July, where the cycle was:

//10 secs on//2 secs off//10 secs on//2secs off//10 secs on//2 secs off//10 secs on//2 secs off//10 secs on// 122 secs off//

The on period coincides with the exact time of UT and then, every 3 minutes (example with the cycle of 20 seconds on and 160 seconds off: heater on from 08:00:00 UT until 08:00:20 UT, then heater off from 08:00:20 UT to 08:03:00 UT when a new on cycle would start). Consequently the overshoot effect (theory in section 3.5.2) is present in the measurements.

Apart from the overshoot, some interesting events observed in the spectrograms were a possible spectral width variation during the heating cycles, fast Doppler velocity reversals and some evidences of PMSE layers modulated by gravity waves.

It would be interesting for the reader to check the spectrograms that have been produced for all the hours of data and to compare them, at the same time, with the different observations that I mention in the next sections. This could be done by looking in the examples of section 5.3 (only some of them), or better by using the CD-ROM attached to the thesis where all the plots produced are available.

The next sections are divided in the different days of the EISCAT campaign from the 5th of July 2004 until the 15th of July 2004 (excluding the 9th of July where no data was taken).

6.2 THE 5th OF JULY

-The radar was operating from 06:52 to 11:12 UT. (Figure 5.2 shows from 07:00 to 08:00 UT).

-The gates produced are from 81 Km to 89.4 Km altitude.

Before 07:20 UT, only a very thin PMSE layer (around 1 Km) is observed with maximum SNR values of 21 dB and with a narrow spectra, maximum Doppler velocity of ± 15 m/s. From this time until 11:12, a PMSE layer is observed going from 83 Km to 87 Km altitude approximately, reaching SNR around 32 dB at different altitudes, and a maximum Doppler velocity of ± 45 m/s at 08:22 UT, between 84.3 and 85.5 Km approximately.

The heater effect is very clear during this day. While the heater is on, it is possible to observe a spectral power decrease. When it is turned off, the spectral power increases to a value higher than it was before the heater was on; it is the overshoot effect (Figure 3.3). When the spectral power is not very high compared to the background noise (SNR around 12 dB), we observe how, when the heater is on, the echo almost disappears (taking approximately noise values). The next figure is an example of this event:

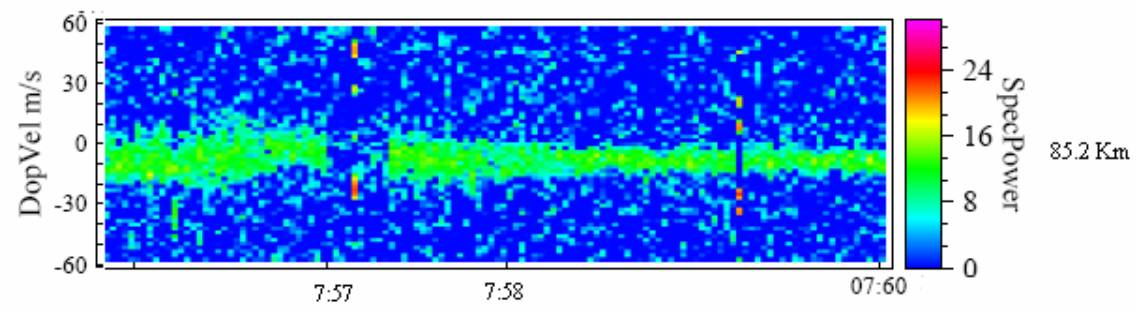

Figure 6.1→ Spectrogram produced for the altitude region 85.2 km during the PMSE experiment, carried out on 5th July 2004 from 07:56 to 08:00 UT. From 07:57:00 to 07:57:20 the heater was on.

Although the heater effect is very clear during the whole day, in the last one hour of measurements, in a thin layer of PMSE at 89 Km altitude, the same effect is not present.

In this day was also observed two very interesting events in the spectral nature of the PMSE:

-A frequency jump in a very short period of time occurs at 08:21:30 UT approximately with its corresponding change in Doppler velocity (see figure 6.2). In section 7.3 it will be shown in detail.

- According to the recent theories about PMSE, the electron heating should not affect the PMSE spectral width (it should affect only the strength, see theory in section 3.5.3). But in some of the spectrograms produced, it is possible to see some changes that could be produced by the heating of the electrons, since these changes are occurring while the heater is on and when it is just turned off (see figure 6.2). In section 7.2.3 it will be discussed.

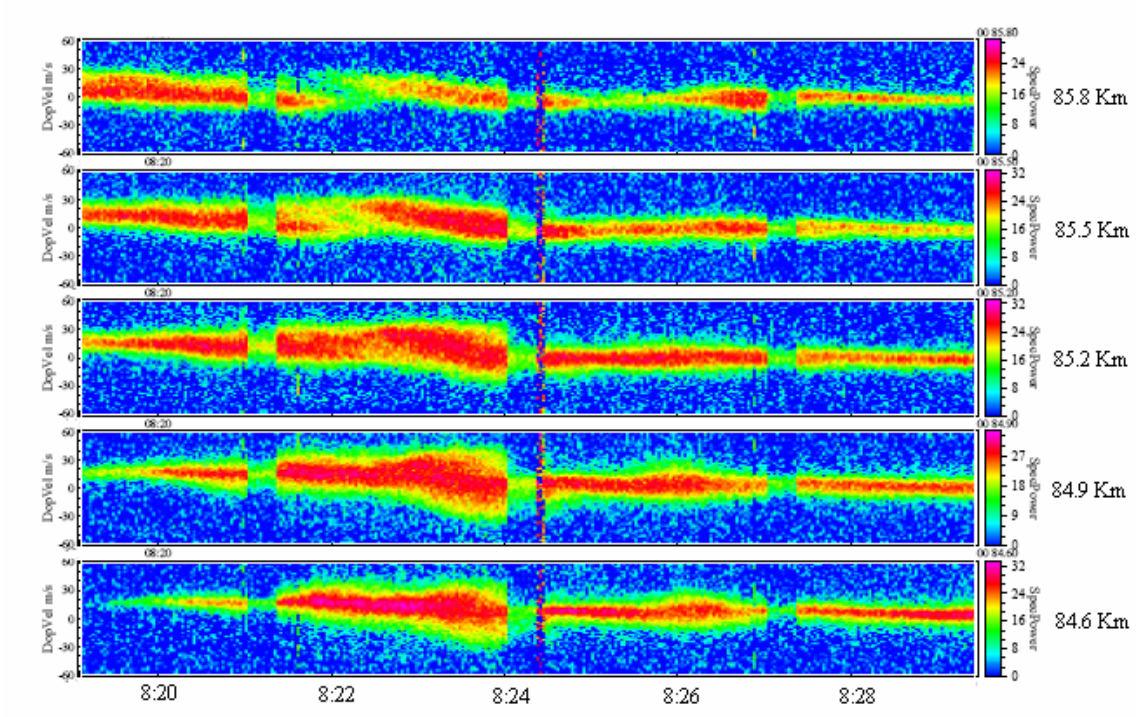

Figure 6.2→Spectrogram produced for 5 gates with altitudes between 84.6 and 85.8 km during the PMSE experiment, carried out on 5th July 2004 from 08:19 to 08:30 UT. In this figure it is possible to observe the two events mentioned above.

6.3 THE 6th OF JULY

-The radar was operating from 07:00 to 11:00 UT.

-The gates produced are from 80.7 Km to 89.1 Km altitude.

During all the measurements of this day, a thick PMSE layer is observed appearing in almost all the gates produced, with maximum SNR values of approximately 32 dB in different altitudes and periods of time, and with a narrow spectra, Doppler velocity around $\pm 15 m/s$. An increasing in its spectra is also noticed for the period of time within 07:28 and 08:08 UT and between 85.8 and 88.5 Km altitude, reaching Doppler velocity values of $\pm 40 m/s$.

The heater effect in this day, between 07:00 and 08:00 UT, is not observed (at least not like in the next hours, especially in the highest gates); but it reappears from 08:00 to 11:00 UT.

As the 5th of July, the spectra seems to change in some gates during the heating period. Since this event is usually observed in all our spectrograms produced, it will not be mentioned again until the analysis in section 7.2.3.

6.4 THE 7th OF JULY

-The radar was operating from 06:55 to 11:08 UT.

-The gates produced are from 80.7 Km to 89.1 Km altitude.

Like the 6th of July, PMSE is observed in almost all the gates produced, but with the difference that in this day, it shows a multilayer structure (see figures 6.3 and 6.4):

-From 06:55 to 08:05 UT, two layers of PMSE. One between 85.8 and 89.1 Km altitude with maximum SNR of 22dB and the other between 83.1 and 85.2 Km altitude with maximum SNR of 27 dB, both with a narrow spectra and Doppler velocity around $\pm$ 15 m/s.

-From 8:05 to 10:00 UT, the two layers merge into one thick layer that goes from 82 to 90 Km altitude with approximately maximum SNR of 32 dB and spectra values as the layers before.

-At the end of the measurements, from 10:30 to 11:08 UT, this thick layer is again divided, this time in three layers at the upper, middle and bottom gates (between 88 - 92, 86.4 - 87.6 and 81 – 84 Km altitude respectively) with approximately the same SNR and spectra values as the thick layer before.

An interesting characteristic of this day is that, unlike the other days, the heater effect is barely noticeable during all the measurements.

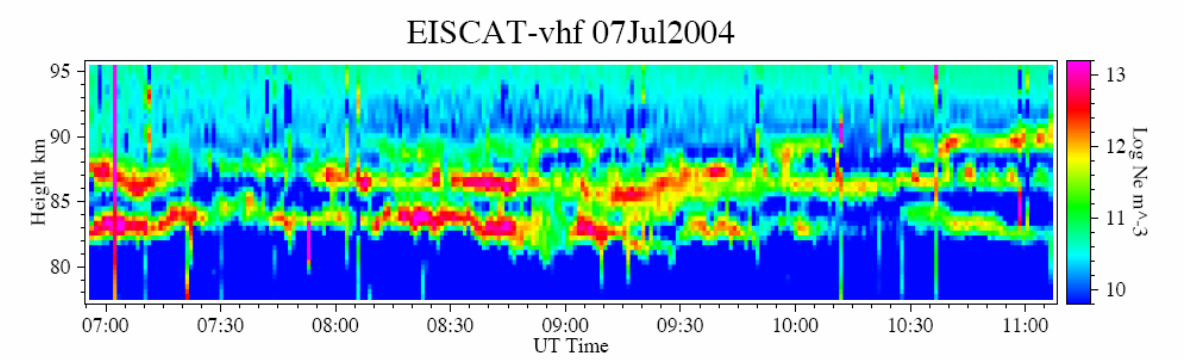

Figure 6.3→ Ne map produced for the altitude region 77-95 km during the PMSE experiment, carried out on 7th July 2004 from 07:00 to 11:30 UT. In this type of plot is also observed the multilayer structure of PMSE during this day.

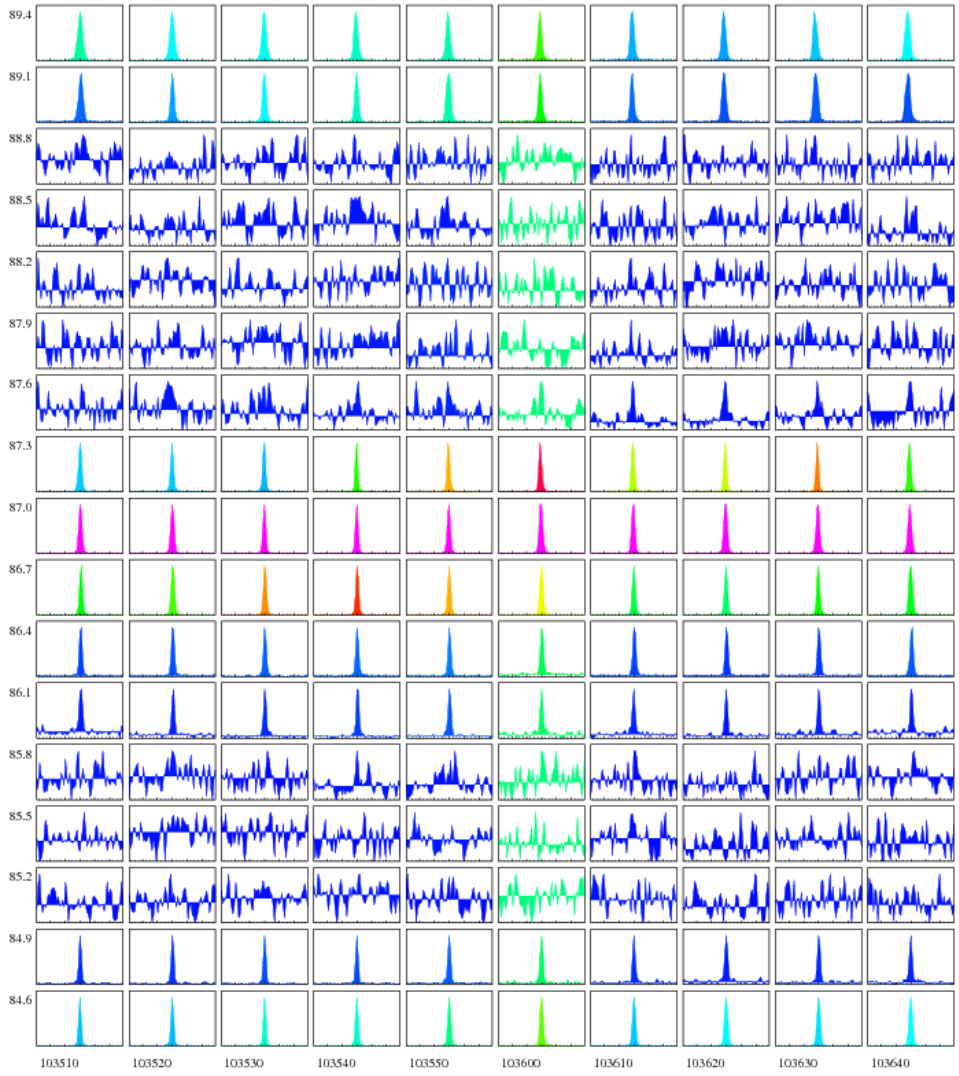

Figure 6.4→ spectral plot with 17 gates from 84.6 to 89.4 Km altitude and an integration time of 10 seconds, during the PMSE experiment, carried out on 5th July 2004 from 10:35:10 to 10:36:40 UT.
3 PMSE layers are observed in this plot, which are separated with noisy gates.

6.5 THE 8th OF JULY

-The radar was operating from 07:00 to 10:00 UT.

-The gates produced are from 81.6 Km to 90 Km altitude.

Only a very thin layer of PMSE is observed between 81.3 and 82.9 Km along all the time that the radar was working, with very narrow spectra, average Doppler velocity around $\pm 5 m/s$ and also a low SNR with a maximum of 18 dB.

With this low SNR, when the heater is on, PMSE disappears as a consequence of the electron heating.

Note: The next section is 10th of July because there is no data from the 9th July.

6.6 THE 10th OF JULY

-The radar was operating from 07:00 to 11:16 UT.

-The gates produced are from 80.1 Km to 89.4 Km altitude.

From 07:30 to 09:20 UT, a thick PMSE layer is visible between 81 and 86.7 Km, with narrow spectra, average Doppler velocity around $\pm 10 m/s$ and a maximum SNR of 30 dB approximately. After 09:20, PMSE appears at two different altitudes, between 86.4 and 90 Km and between 81.3 and 83.7 Km, with similar SNR and Doppler velocity values than before.

The heater effect has a variable intensity. For instance, between 08:00 and 10:00 UT, this effect is practically insignificant.

Between 08:37 and 08:47 UT and from 81 Km to 82.5 Km altitude, the PMSE signal seems to be modulated by a gravity wave, oscillating vertically. But the wave progression is only observed during this interval of time which creates me some doubts whether or not it is a real signature of gravity wave.

6.7 THE 11th OF JULY

-The radar was operating from 07:05 to 11:34 UT. (Figure 5.3 shows from 07:00 to 08:00 UT).

-The gates produced are from 79.8 Km to 90.9 Km altitude.

Two layers of PMSE appear this day. One is observed since the beginning of the measurements, until 8:30 UT, between 84 and 87 Km altitude, with a maximum SNR of 24 dB and maximum Doppler velocity of ± 30 m/s. The other layer goes from 07:50 to 10:30 UT, between 83.1 and 85.2 Km altitude, with a maximum SNR of 20 dB and very narrow spectra, maximum Doppler velocity around ± 20 m/s.

The heating cycle used for this day was:
//10 secs on//2 secs off//10 secs on//2secs off//10 secs on//2 secs off//10 secs on//2 secs off//10 secs on// 122 secs off//

The heater effect is observed in both layers during all the measurements, being possible to see the five overshoots in each cycle, one in each part of the cycle where the heater changes from on to off. Figure 6.5 shows this event.

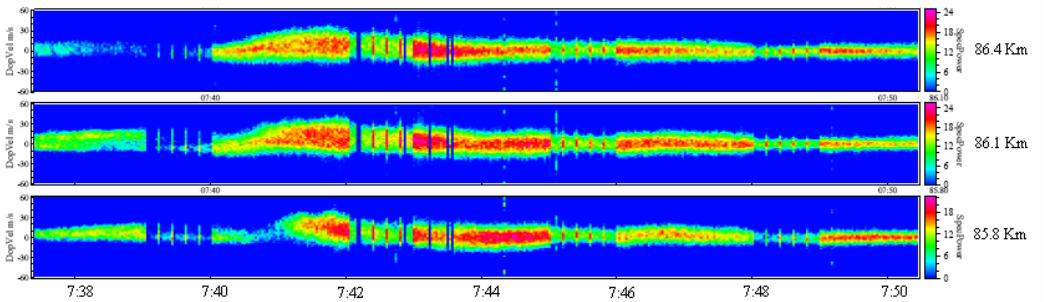

Figure 6.5→ Spectrogram produced for 3 gates with altitudes between 85.8 and 86.4 km during the PMSE experiment, carried out on 11th July 2004 from 07:36 to 07:51 UT.

6.8 THE 12th OF JULY

-The radar was operating from 06:45 to 11:32 UT.

-The gates produced are from 80.10 Km to 88.20 Km altitude.

PMSE appears during the whole time in one layer, which goes first, varying between 81 and 84.6 Km altitude from 06:45 to 08:30 UT with maximum SNR values around 28 dB and with a narrow spectra, Doppler velocity around $\pm 10 m/s$. Then from 8:30 to 11:20 UT, it varies between 81.3 and 85.8 Km altitude, with maximum SNR values around 28 dB and with a spectra that varies quantitatively from the upper gates to the lower gates. See next figure:

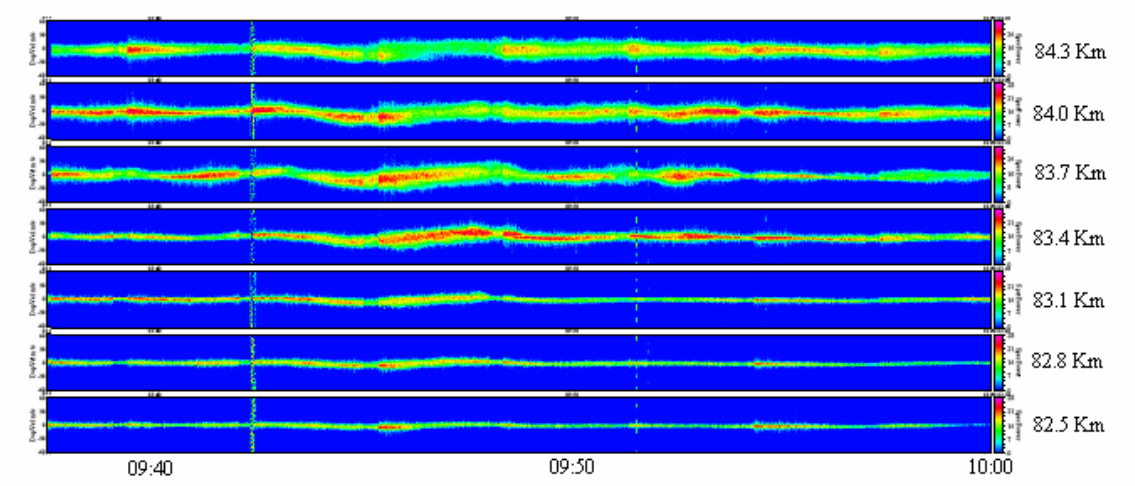

Figure 6.6→ Spectrogram produced for 7 gates with altitudes between 82.5 and 84.3 km during the PMSE experiment, carried out on 12th July 2004 from 09:38 to 10:00 UT. In the upper gates are observed Doppler velocities that reach ± 25 m/s while in the bottom gates the Doppler velocity is around ± 10 m/s.

Also between 08:22 and 09:00 UT, PMSE is observed out of the main layer in a range of altitudes between 86 and 88.2 Km with a maximum SNR of 20 dB and a maximum Doppler velocity of ± 25 m/s.

The heater effect in this day is barely observed as can be noticed for instance in figure 6.6.

6.9 THE 13th OF JULY

-The radar was operating from 06:50 to 11:21 UT. (Figure 5.4 shows from 08:00 to 09:00 UT).

-The gates produced are from 81.3 Km to 89.7 Km altitude.

PMSE appears, in all the time measured, in one layer which goes:

-First, varying between 83.70 and 86.40 Km from 06:50 to 07:50 UT with maximum SNR values around 20 dB and with a narrow spectra, Doppler velocity around $\pm 15 m/s$.

-Between 07:50 and 09:30 UT, the layer becomes thicker and it varies from 81.3 up to 88.80 Km altitude (PMSE has this large thickness exactly at 08:30 UT) with maximum SNR values around 36 dB and with a spectra that varies quantitatively from the upper gates (maximum Doppler velocity equal to ± 50 m/s) to the lower gates (maximum Doppler velocity ± 15 m/s).

Between 08:00 and 10:00 UT, several fast Doppler velocity reversals take place. One very clear example of this event occurs at 08:32 UT and will be analysed in section 7.3.

Also between 08:00 and 10:00 UT, some of the best candidates to be signatures of gravity waves are observed, especially at 08:30 UT. It will be discussed in section 7.4.

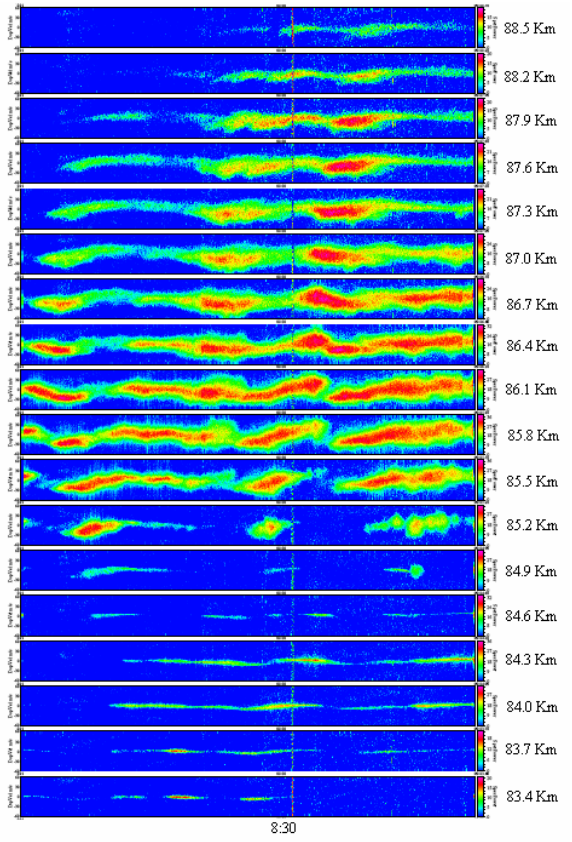

Figure 6.7→ Spectrogram produced for 18 gates with altitudes between 83.4 and 88.5 km altitude during the PMSE experiment, carried out on 13th July 2004 from 08:22 to 08:37 UT. In the upper gates are observed Doppler velocities that reach ± 50 m/s while in the bottom gates the Doppler velocity is around ± 8 m/s.
At 08:32 UT a Doppler velocity reversal takes place at altitudes around 86.1 Km.
It is also observed some evidences of PMSE modulated by a gravity wave (the progression of the signal through the different gates).

-Between 09:30 and 11:21 UT, the layer comes back to a similar shape than it is from 06:50 to 07:50 and with similar values of SNR and Doppler velocity.

The heater effect, as the day before, is not clearly observed.

6.10 THE 14th OF JULY

-The radar was operating from 06:47 to 11:00 UT. (Figure 5.5 shows from 09:00 to 10:00 UT).

-The gates produced are from 80.10 Km to 88.80 Km altitude.

In this day, strong echoes are observed in almost all the gates, but the strongest signals received are concentrated between 82 and 86 Km altitude reaching maximum values of SNR of 40 dB at 9:30, which are the highest values received during the campaign. The average Doppler velocity this day is around ± 10 m/s but, like the days 12th and 13th of July, between 9:10 and 10:40 UT, there is a big difference in this velocity: the upper gates have a larger Doppler velocity with values around ± 30 m/s while in the bottom gates it conserves the same as before, around ± 10 m/s.

Like the 13th of July, evidences of gravity waves are observed between 08:00 and 09:00 UT. Also several frequency jumps take place during this hour but with lower discontinuities of the vertical velocities than in the cases reported the day before.

The heater effect continues not being clear during this day.

6.11 THE 15th OF JULY

-The radar was operating from 06:47 to 12:00 UT.

-The gates produced are from 80.00 Km to 88.50 Km altitude.

PMSE appears from 07:00 to 12:00 UT, and between 83.10 and 86.10 Km altitude approximately. The power signal received is not very strong, with an average SNR around 15 dB and a narrow spectra, with Doppler velocities not reaching $\pm$ 10 m/s. But between 08:40 and 10:30 UT, an increase on PMSE thickness is observed, varying between 81.9 and 87.3 Km altitude approximately. And at 08:56 UT and 84.6 Km altitude, the power and Doppler velocity increase and reach 25dB and ± 20 m/s respectively.

The heater effect is observed clearly again during this day, and in some cases, as the 5th of July, PMSE takes noise power values while the heater is on.

CHAPTER 7

DETAILED STUDY OF PMSE EVENTS

7.1 INTRODUCTION

This chapter will deal with the analysis and explanation of the most interesting events observed in PMSE, which were found and reported in the general observation, chapter 6.

Thanks to the heater facility, new characteristics of PMSE have been discovered, some of them are well understood but others are still under discussion. In section 7.2, we will analyse different effects on PMSE caused by the two different heating cycles used during the EISCAT campaign with special attention to spectral measurements that are analyzed for the first time with regard to heating effects. The measurements will be compared and contrasted with the models and theory previously studied. The types of events observed on PMSE during the heating cycles that will be analysed are:

- Overshoot effect using the cycle of 20 secs on and 160 secs off.
- Overshoot effect using very short cycles of heater on and heater off.
- The possibility of a correlation between the spectral width and the heating cycles.

Section 7.3 will discuss frequency jumps. This event has been observed in PMSE spectrograms since the first studies (Röttger, J., La Hoz, C., Franke, S., J., Liu, C.H., 1990) and several models have been proposed to explain it. In this section, we will apply these models to our PMSE measurements to study which one fits better with our frequency jumps. A possible connection with gravity waves seems to be a good option of these models, especially for the frequency jumps observed the 13th of July where the clearest signatures of gravity waves were found above the frequency jumps. Some characteristics of the gravity waves observed the 13th of July will be studied in section 7.4.

7.2 EVENTS CAUSED BY THE HEATING

7.2.1 Overshoot effect

In the spectrograms, lots of examples were found, in which PMSE follows the Havnes (Havnes et. al 2003) predictions for the heating cycle of 20 seconds on and 160 seconds off.

Now we will study one of these examples, for instance the 5th July 2004 at 10:18 UT and at 84.9 Km altitude. The values of the spectral power calculated by fitting Gaussian functions to the spectra, will be compared with the observations in the spectrograms.

Figure 7.1 shows the typical effect that the electron heating causes over PMSE. We describe now these effects:

Figure 7.2 shows, with the highest possible time-resolution, the spectra from 4 seconds before the heater was on, until 4 seconds after it was off (30 seconds total).

Here is the summary of the events observed in this figure:

-Until 10:18:00 UT, the maximum spectral amplitude value (in arbitrary units) is 200.

- At 10:18:02 (the first sample with heater on), the amplitude decreases to 30 (6.7 times lower), and conserves a low value (between 30 and 80) until 18:10:20 (the last sample with heater off). During these 20 seconds, a little increase in power is noticed.

- At 10:18:22 (the first sample after the heater is off again), the amplitude increases up to 300, which is called the overshoot (in this example it is not very strong).

In the next 160 second, the power comes back to the values before the heater was on. Figure 7.3 shows the spectral power variation from 10:17 to 10:19 UT. To verify the Havnes prediction using heating cycles, we can compare this figure with figure 3.4 (section 3.5.2).

By looking at figure 7.1, it is noticed an apparent narrowing of the spectral width during the 20 seconds with the heater on. This event is not confirmed in figure 7.2. Also figure 7.4 have been produced, in which we see how the spectral width varies with time during two cycles of heating, and the result is the same, the spectral width does not change while the heater is on. Thus we found that the spectral width decrease observed in figure 7.1 is due to the way the spectrograms, Power vs Doppler velocity-time, have been done, the logarithmic scale used makes this effect in the plots when a intensity variation occurs, like in this case, the expected power decreased during the heating cycle. It does not mean that the possibility to find this correlation between heating cycles and spectral width is ruled out, but it is unlikely. Section 7.2.3 will study this possible correlation with more detail.

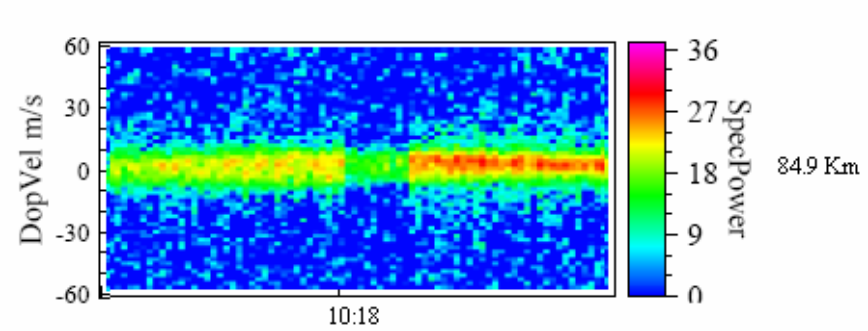

Figure 7.1→ Spectrogram produced for the altitude region 84.9 km during the PMSE experiment, carried out on 5th July 2004 from 10:17 to 10:19 UT. From 10:18 :00 to 10:18:20 the heater was on.

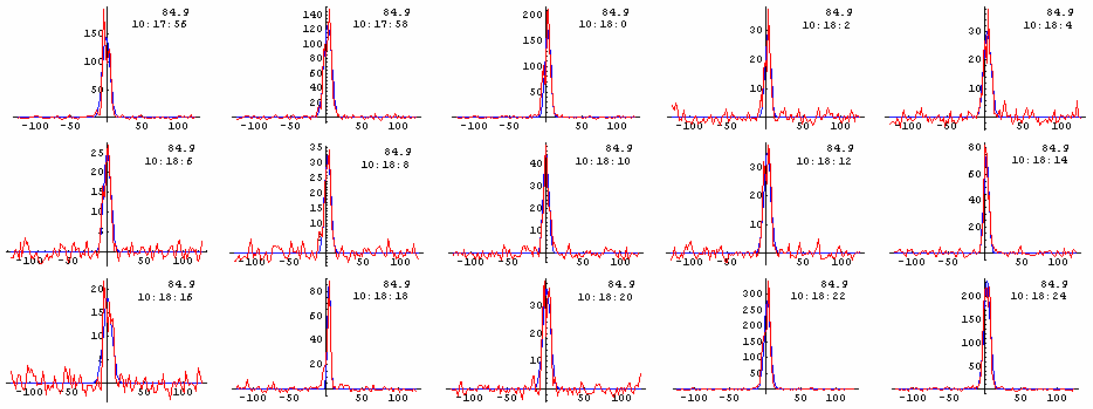

Figure 7.2→ PMSE spectra from 10:17:56 to 10:18:24 UT at 84.9 Km altitude. Between 10:18:00 and 10:18:20 UT the heater was on. Integration time of 2 seconds.

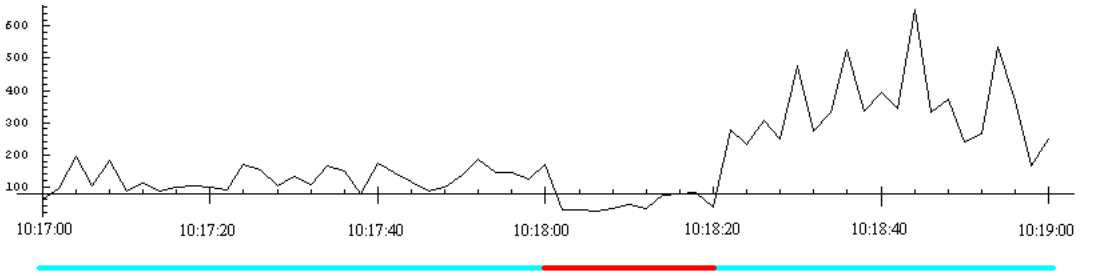

Figure 7.3→ Spectral power variation from 10:17:00 to 10:19:00 UT at 84.9 Km. From 10:18:00 to 10:18:20 UT the heater was on, and just after it is observed the overshoot. The red and blue lines below the time show when the heater was on and off respectively.

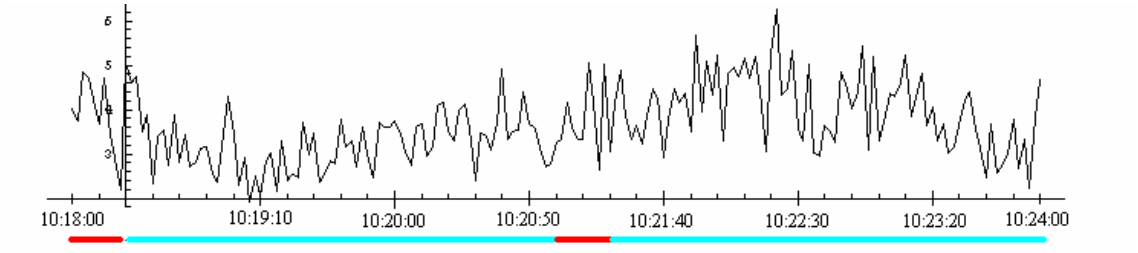

Figure 7.4→ Spectral with variation of two heating cycles from 10:18:00 to 10:24:00 UT at 84.9 Km. The red and blue lines below the time show when the heater was on and off respectively.

7.2.2 Overshoot effect using short cycles of on and off.

In section 6.7, we reported a different heating cycle used during the 11th of July. The heating cycle used was:

//10 secs on//2 secs off//10 secs on//2secs off//10 secs on//2 secs off//10 secs on//2 secs off//10 secs on// 122 secs off//

The aim of this cycle was to study how large it is possible to increase PMSE spectral power by heating the electrons during short and consecutive intervals of time. Therefore the interesting part of the cycle is where the 5 overshoots are observed (the next 122 seconds are used to leave the dusty plasma comes back to the undisturbed conditions).

One of the gates with the highest spectral power received is at 86.1 Km altitude between 08:00 and 09:00 UT, three heating cycles of it are shown in Figure 7.5.

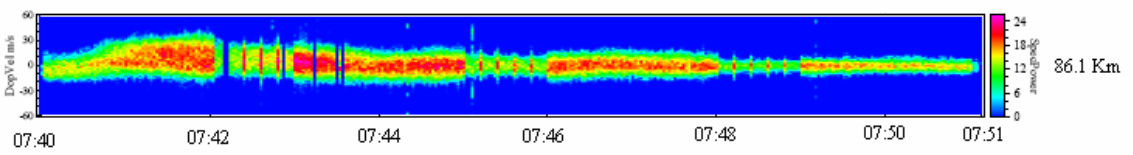

Figure 7.5→ Spectrogram produced for the altitude region 86.1 km during the PMSE experiment, carried out on 5th July 2004 from 07:40 to 07:51 UT.

In the first cycle represented in figure 7.5, there are some time intervals where PMSE disappears (07:42 UT), this event does not have anything to do with PMSE, it is only due to the loss of some information in the measurements. Figure 7.6 shows this lost data:

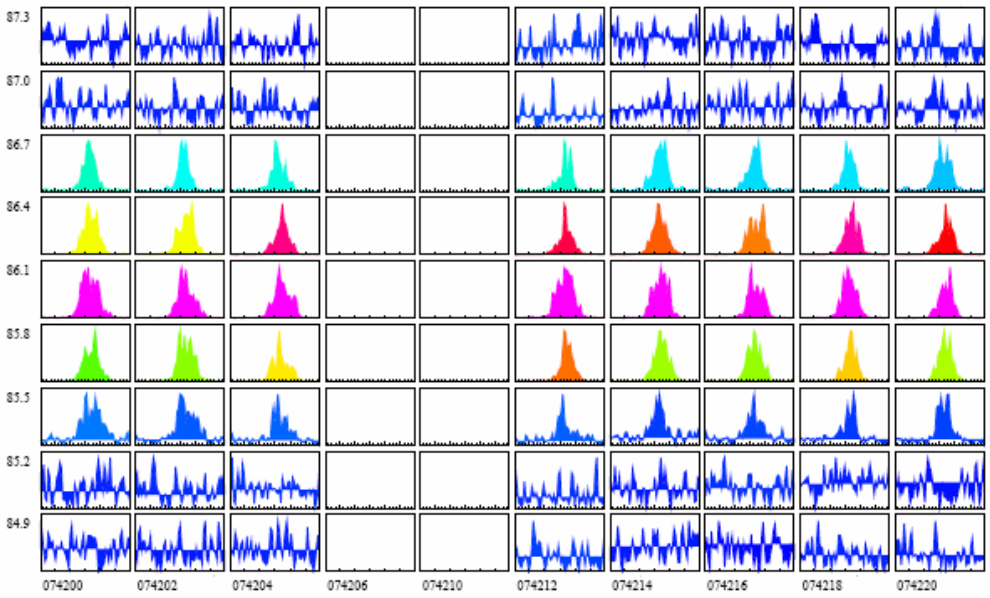

Figure 7.6→ PMSE spectral plot with 9 gates from 84.9 to 87.3 Km altitude and an integration time of 2 seconds, during the PMSE experiment, carried out on 1st July 2004 during the heating cycle from 07:42:00 to 07:42:20 UT. Data from 07:42:06, 07:42:08 and 07:42:10 UT does not exist.

Back to the mentioned experiment with the heating cycle, the idea was to see if it was possible to increase the magnitude of each overshoot with respect to the previous one until a maximum limited by the heating. Figure 7.7 shows the overshoots of the three heating cycles mentioned before plus an additional one:

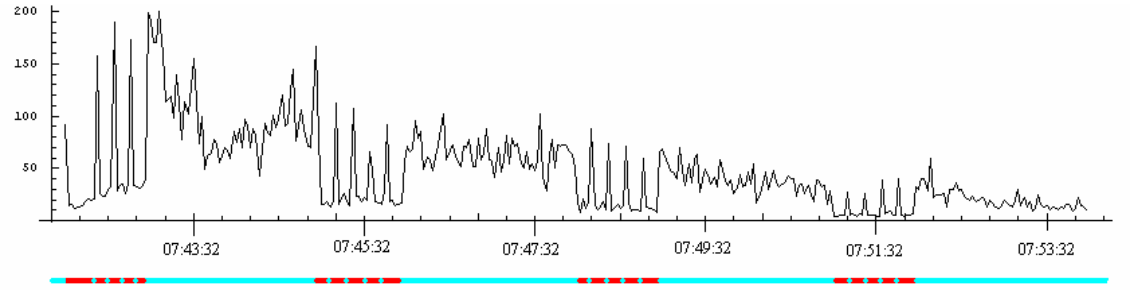

Figure 7.7→ Spectral power variation from 07:42:00 to 07:54:00 at 86.1 Km. altitude.. The red and blue lines below the time show when the heater was on and off respectively.

By analysing the spectral power of, for instance, the two first groups of five overshoots, we see that:

-1st group→ the first overshoot is not observed due to the lost information, and the others are $2^o < 3^o > 4^o < 5^o$.

-2nd group→ $1^o > 2^o > 3^o < 4^o < 5^o$.

We notice that the pattern of overshoots increasing is not observed, one cause is that during the heating process, some electrons are absorbed so the electron density decreases (in section 3.2 we saw that a electron density decrease implies a lower PMSE) but, in this case, the main reason is a natural decrease on PMSE, which can be observed during this period of time. It was bad luck that we made this attempt when PMSE had a tendency to decrease steadily in time.

The above mentioned absorption of electrons during the heating has also been observed with the heating cycle of 20 seconds on and 160 off. During the 20 seconds on, in theory, PMSE power should increase slowly until the overshoot but, sometimes, a power decrease is observed before the overshoot, which is caused by this electron absorption.

7.2.3 Possible correlation between spectral width of PMSE and the heating cycles

In this section, we are going to follow the same steps as in section 7.2.1 but, with one of the examples observed where the spectral width seems to change with the heating cycles.

The possible correlation that I was trying to find between the spectral width and the heating cycles observed in the spectrograms Power vs Doppler velocity-time is represented by the following diagram:

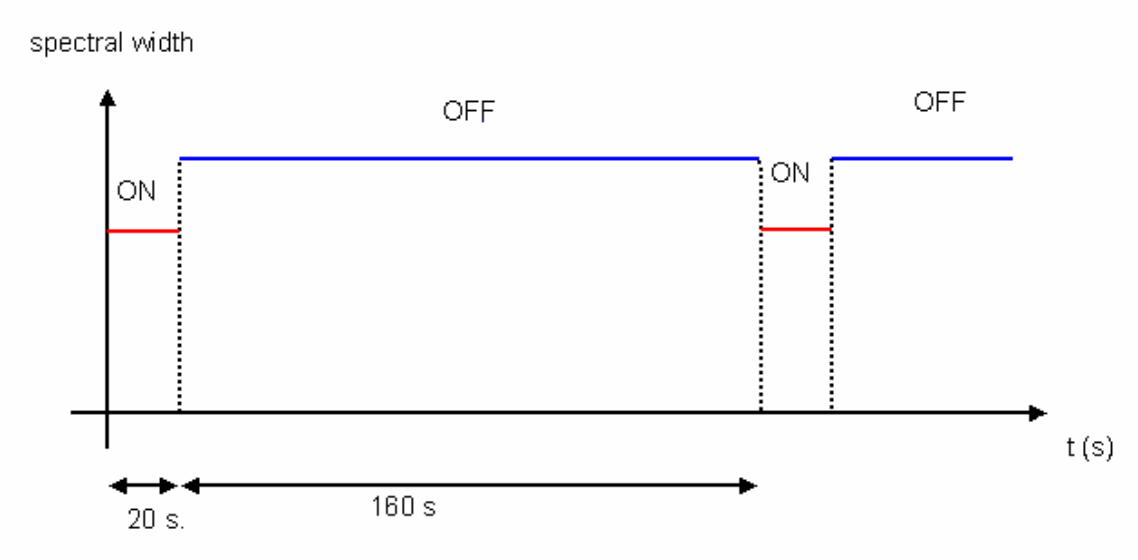

Diagram 7.1→Diagram of the spectral width vs time which shows the possible correlation observed between the spectral width and the heating cycles. The red and blue lines shows the possible spectral width values when the heater is on and off respectively.

In this case, the 5th of July, where the heater starts the on period at 8:21 and at 8:24 UT (figure 7.8) will be analysed.

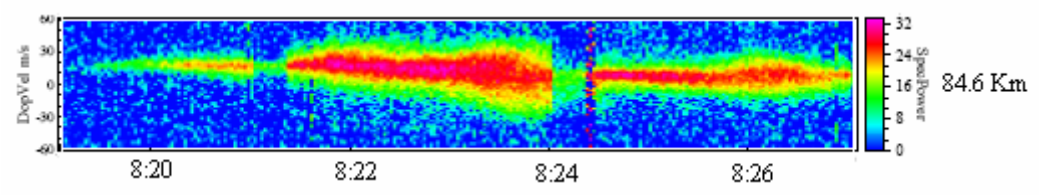

Figure 7.8→ Spectrogram produced for the altitude region 84.6 km during the PMSE experiment, carried out on 5th July 2004 from 08:19 to 08:27 UT.

Figure 7.9 shows the spectra from 4 seconds before the heater was on until 4 seconds after it was off.

Figure 7.10 shows the spectra from 4 seconds before the heater was on until 14 seconds after it was off (here I did 14 more seconds due to the noisy signal received after the heater was off).

In both figures the overshoot is observed stronger than in the example in section 7.2.1 but, what is very interesting is how the Doppler velocity varies with the time.

By looking at figure 7.11, which shows the two heating cycles of figure 7.8, we notice how, after the first 20 seconds with the heater on (at 08:21:20), the spectral width increases. During the second heating period, the same event is observed at 08:24:20 UT and it decreases again before the next heating cycle. It does not follow the pattern of diagram 7.1. It seems to be natural spectral width variations not related to heating.

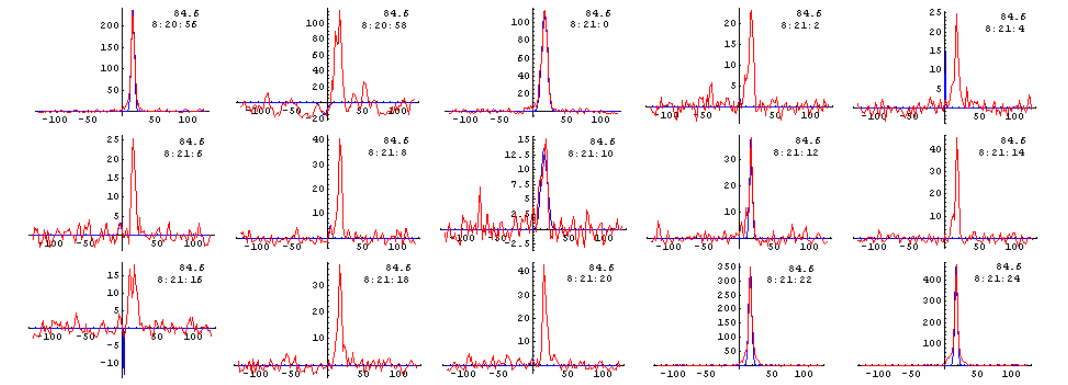

Figure 7.9→ PMSE spectra from 08:20:56 to 08:21:24 UT at 84.6 Km. Between 08:21:00 and 10:21:20 UT the heater was on. Integration time of 2 seconds.

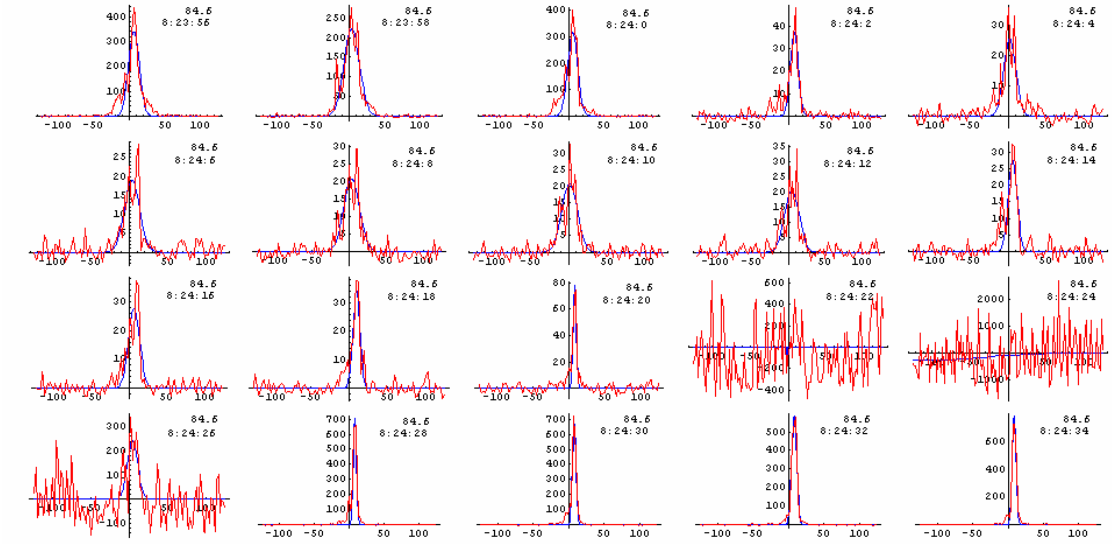

Figure 7.10→ PMSE spectra from 08:23:56 to 08:24:34 UT at 84.6 Km. Between 08:24:00 and 08:24:20 UT the heater was on. Integration time of 2 seconds.

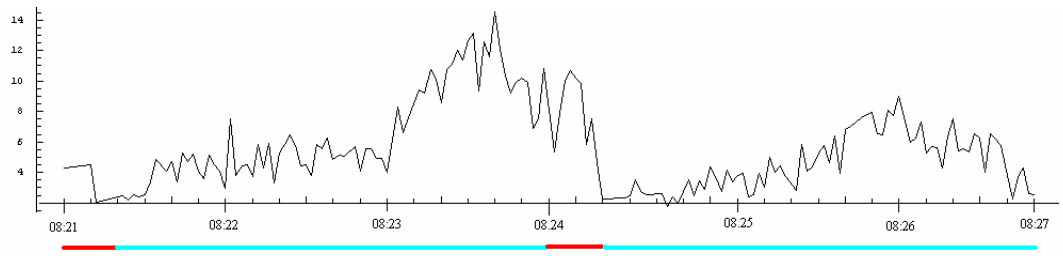

Figure 7.11→ Spectral with variation of two heating cycles from 08:21:00 to 08:27:00 UT at 84.6 Km. The red and blue lines below the time show when the heater was on and off respectively.

After this example where no correlation was found, other periods of time were tested. The 5th of July from 07:00 to 08:00 UT, I found some examples which made me doubt about the possibility of this correlation but, as I am going to explain, it was ruled out. Figure 7.12 shows the spectrograms of two gates (85.2 and 84.9 Km) from this day.

Spectral with variation plots of two heating cycles were produced for the next interval of time in the two adjacent gates:

-5th of July 2004 from 07:51:00 to 07:57:00 at 84.9 Km (figure 7.13)

-5th of July 2004 from 07:51:00 to 07:57:00 at 85.2 Km (figure 7.14)

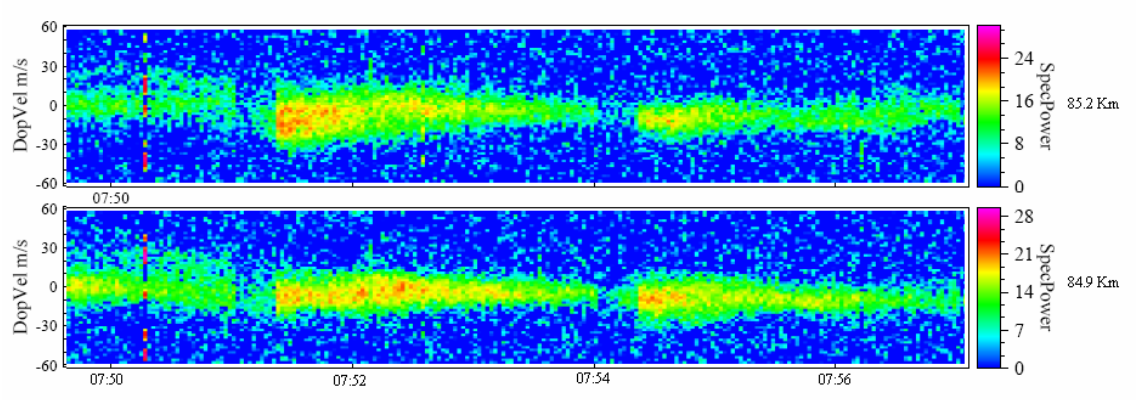

Figure 7.12→ Spectrogram produced for 2 gates with altitudes 84.9 and 85.2 km during the PMSE experiment, carried out on 5th July 2004 from 07:50 to 07:57 UT.

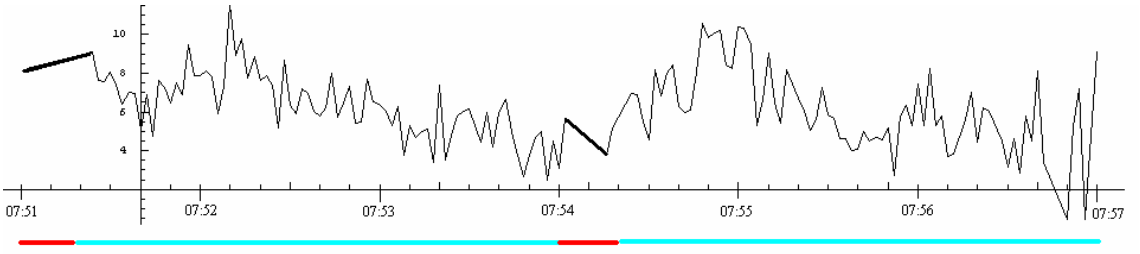

Figure 7.13→ Spectral with variation of two heating cycles from 07:51:00 to 07:57:00 UT at 84.9 Km. The red and blue lines below the time show when the heater was on and off respectively.

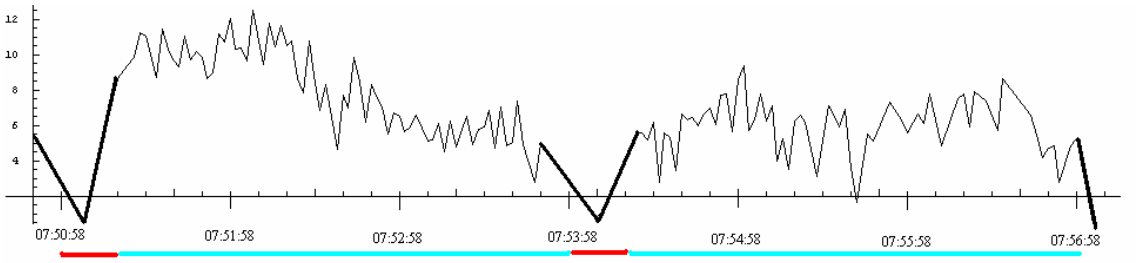

Figure 7.14→ Spectral with variation of two heating cycles from 07:51:00 to 07:57:00 UT at 85.2 Km. The red and blue lines below the time show when the heater was on and off respectively.

Figure 7.14 shows a spectral width variation pattern during the heating cycles as in diagram 7.1 but it is not a valid measurement because, during the heating periods at this altitude, the spectral power of the signal received was very weak (around noise values). When this happens, the program used can not calculate the spectral width and assigns a negative value by default. All these negative values assigned are observed in the spectral width variation plots as straight lines. In figures 7.13 and 7.14, I have marked with a thick black line the spectral width values during the heating time and it coincides with these straight lines.

Figure 7.15 shows the spectral plots from 07:53:54 to 07:54:22 UT at 85.2 Km (the second heating period of figure 7.14) where we can see this effect explained.

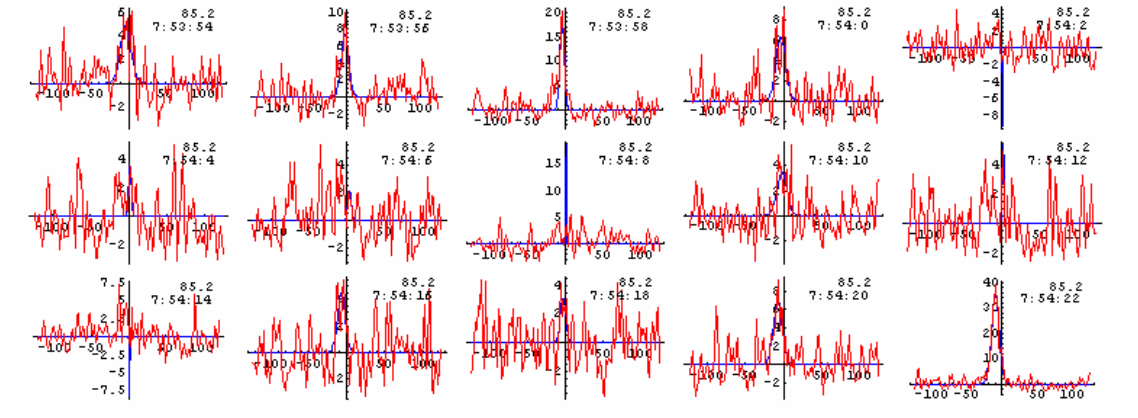

Figure 7.15→ PMSE spectra from 07:53:54 to 07:54:22 UT at 85.2 Km. Between 07:54:00 to 07:54:20 UT the heater was on. Integration time of 2 seconds . It is observe how the signal received during the heating period can not be fitted with the Gaussian function, therefore the spectral width can not be calculated.

A list of conclusions follows:

- The spectral width narrowing observed in the spectrograms Power vs Doppler velocity-time during the heating period was due to the logarithmic scale used to produce these plots.

-The spectral width decrease observed in figures as 7.13 and 7.14 was due to a bad measurement of the spectral width.

- Some real variations of the spectral width during the heating periods were found, but they did not follow a correlation, it was only coincidences between these heating periods and natural variations of the spectral width.

7.3 FREQUENCY JUMPS

7.3.1 Observations and characteristics of frequency jumps

In chapter 6, several frequency jumps in a very short period were reported, the most evident jumps occur the days 5th and 13th of July.

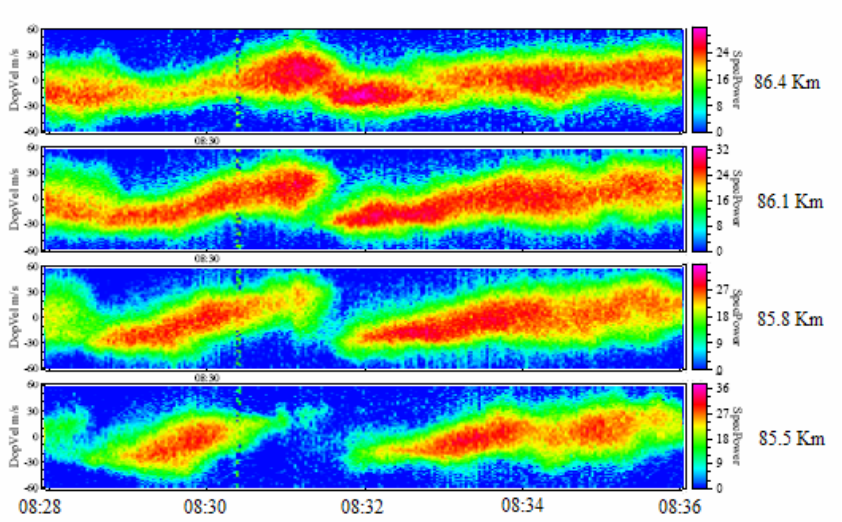

Figure 7.16→ Spectrogram produced for 4 gates with altitudes 85.5 and 86.4 km during the PMSE experiment, carried out on 5th July 2004 from 08:28 to 08:36 UT. A very clear frequency jump is observed at 08:31 UT.

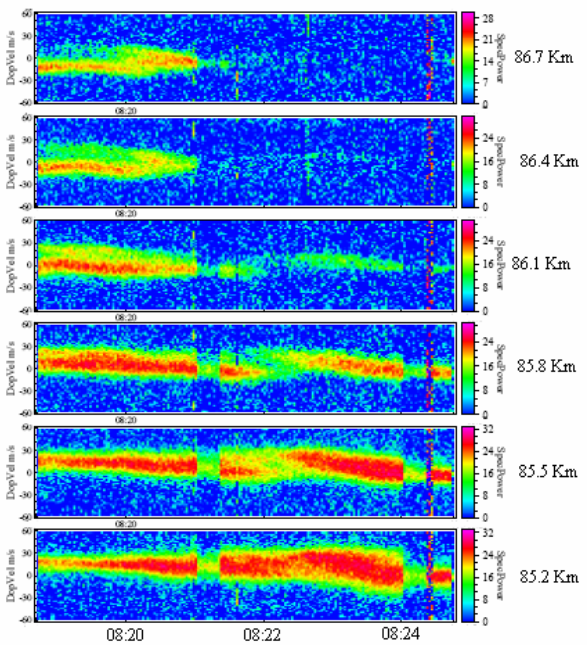

Figure 7.17→ Spectrogram produced for 6 gates with altitudes between 85.2 and 87.6 km altitude during the PMSE experiment, carried out on the 5th July 2004 from 08:19 to 08:25 UT. In the two upper gates, variations of Doppler velocity are observed at 8:20. At 85.8 and 85.5 Km altitude, a Doppler velocity reversal takes place between 08:21:30 and 08:22:30 UT.

This phenomenon has been studied before (Röttger, J., La Hoz, C., Franke, S., J., Liu, C.H., 1990 and Alcala, C. M., Rötger, J. and Kelley, M.C., 1995) where they suggested different models that could explain it.

Figure 7.18 shows a spectrogram produced by La Hoz in 1990 in which frequency jumps are marked with arrows

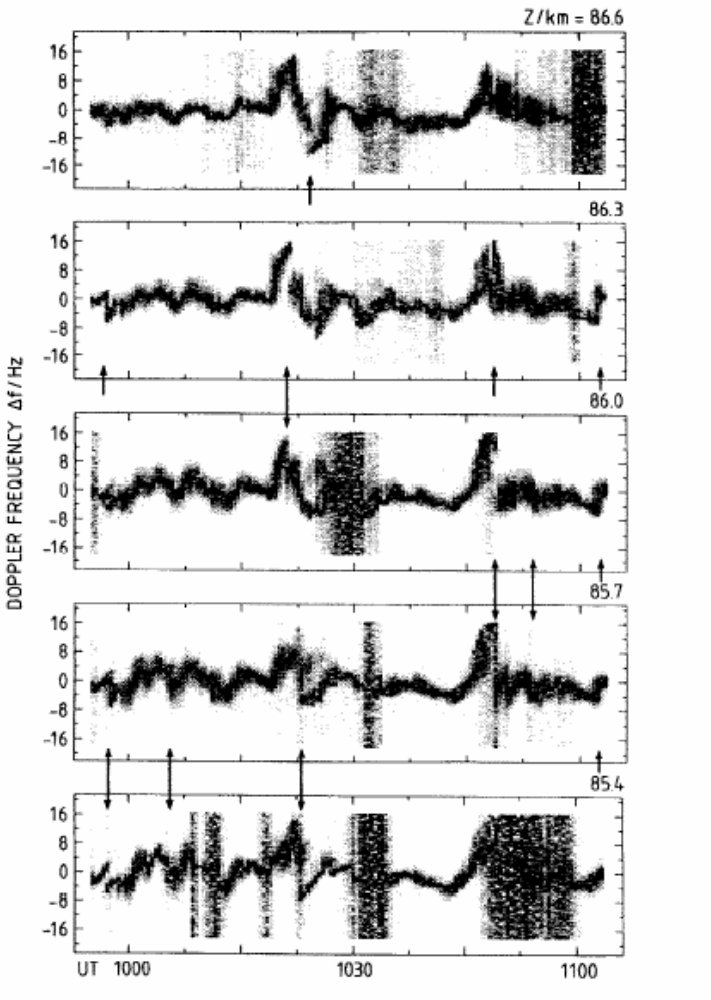

Figure 7.18→ Spectrogram produced for 5 gates with altitudes between 85.4 and 86.6 km with 300 m high resolution, during the PMSE experiment, carried out the 1st of July 1988 (from Röttger, J., La Hoz, C., Franke, S., J., Liu, C.H.,1990)

Some of the characteristics of frequency jumps extract from these previous studies (which can be observed in figure 7.18 and later will be compared with the new measurements of my work) are:

-Frequency jumps frequently occur and with vertical velocity discontinuities that can reach almost 15 m/s.

-The frequency jumps usually occur in less than one minute.

- The velocity change can be positive or negative.

By using plots of Doppler velocity vs time, which use the highest possible time resolution time (2 seconds) we can extract some of the characteristics of the frequency jumps observed in figures 7.16 and 7.17.

Frequency jump of the 13th of July

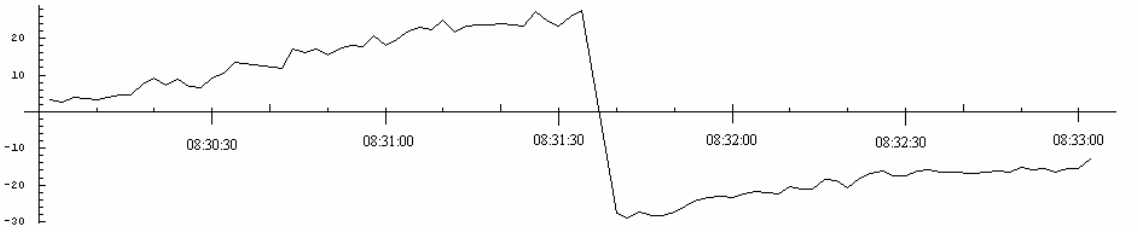

Figure 7.19→ Doppler velocity vs time from 08:30:00 to 08:33:00 UT at 85.8 Km altitude the 13th of July 2004. I chose this altitude because it is the abruptness jump observed.

Figure 7.19 shows a frequency jump where the Doppler velocity jumps from a value of 27.7081 m/s at 08:31:32 UT to a value of -27.8153 m/s at 08:31:38 UT. The straight line that appears in the figure between these two times does not mean a Doppler variation since, by looking at the spectrograms, we see that during this interval of time two spectral peaks appear, and the program used to calculate the Doppler velocity does an average between them (this event of the two spectral peaks will be analysed later in this section since it is the first time that the spectral transition during the frequency jumps has been solved). Thereby the frequency jump implies a discontinuity of the vertical velocity of almost 56 m/s within less than 10 seconds. As we see, the characteristics of this frequency jump are much more extremes than the others observed in previous studies.

Frequency jump of the 5th of July

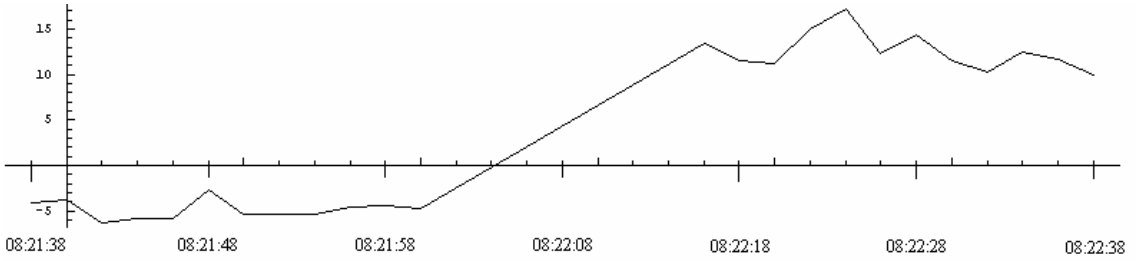

Figure 7.20→ Doppler velocity vs time from 08:21:38 to 08:22:38 UT at 85.8 Km altitude the 5th of July 2004.

Figure 7.20 shows a frequency jump where the Doppler velocity jumps from a value of –5 m/s at 08:22:00 to a value around 14 m/s at 08:22:16 UT, thus ,in this case the discontinuity of the vertical velocity observed is of 19 m/s and it takes place in 16 seconds.

Thanks to the high time resolution used in the last EISCAT campaign (2 seconds), we resolved how the frequency jump occurs, therefore here I explain the analysis done for the frequency jump of figure 7.16 where a new characteristic on the PMSE spectra during the frequency jumps is observed:

In figure 7.21, we see the spectral progression of the signal received.

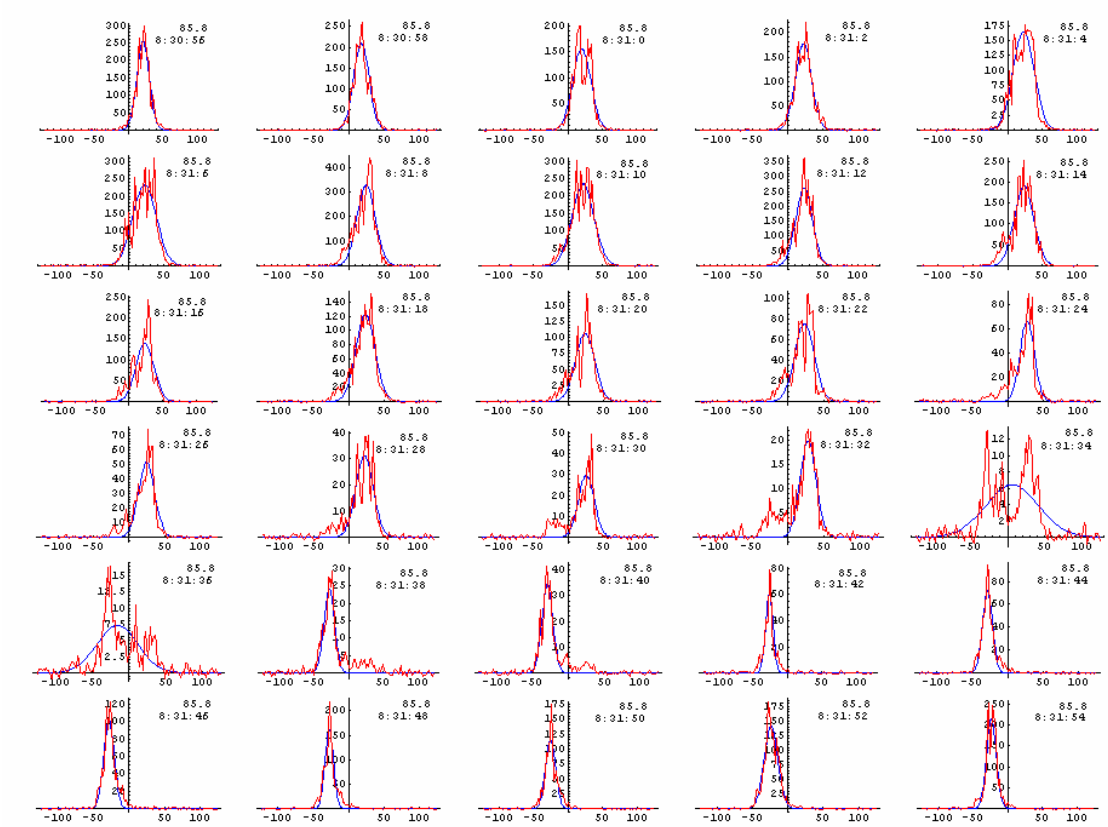

Figure 7.21→ PMSE spectra from 08:30:56 to 08:31:54 UT at 85.8 Km altitude

We observe that before the frequency jump occurs, the Doppler velocity has approximately constant values around 25 m/s. At 08:31:32 it is very clear how a second spectral peak appears with a value of -25 m/s while the other remains in the same position. 2 seconds later, both peaks have the same spectral amplitude and in 2 more seconds the spectral signal located in the positive Doppler starts to disappear. In the next spectral plots, only the spectral signal in the negative Doppler velocities is observed with values around -25 m/s. It is also interesting to see how the spectral power decreases in time, reaching the minimum value just where the two peaks appear, which is in the middle of the frequency jump and after that, it increases again until it reaches the value that it had before the frequency jump.

Figure 7.22 shows in detail the three spectral plots during the frequency jump and we can observe how the Doppler velocity changes from the positive value to the negative value:

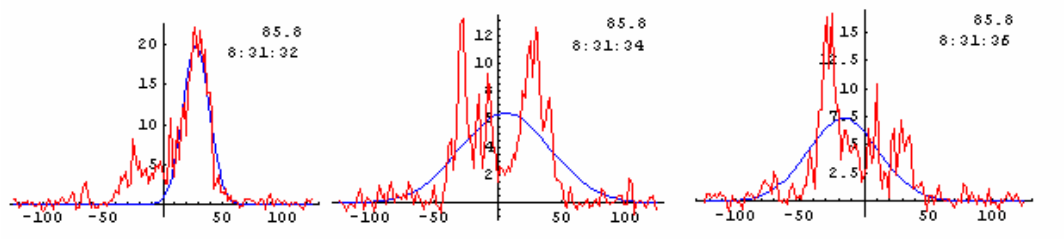

Figure 7.22→ PMSE spectra from 08:31:32 to 08:31:36 UT at 85.8 Km altitude.

7.3.2 Models for frequency jumps

In these previous studies of the frequency jumps, they suggest several models that could solve this event. In the next sections we will see some of the models they proposed and they will be contrasted with the new measurements of the EISCAT campaign in July 2004.

7.3.2.1 Wave steepening

It has been proposed that the frequency jumps are a signature of wave steepening, which occurs when the amplitude of gravity waves increases but breaking into turbulences does not immediately take place (Röttger, J. et al, 1990). See Figure 7.22:

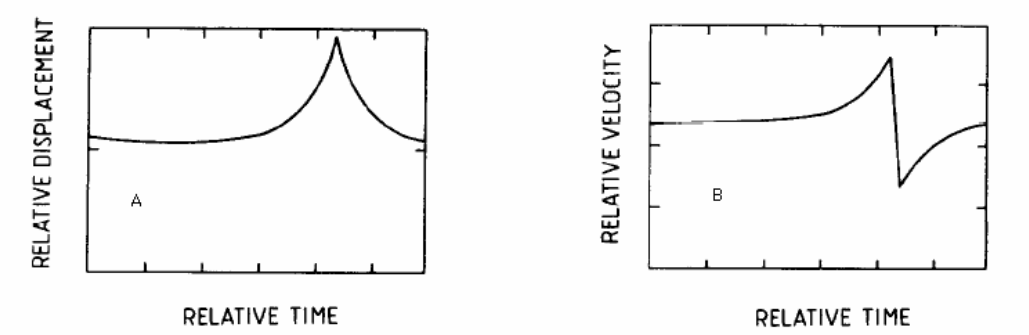

Figure 7.23→ Model surface of a thin layer of turbulence, discontinuity or isentrope in (A) a steepened wave. The corresponding relative velocity (Doppler shift), is shown in panel B. The scales are in arbitrary units. From Röttger, J. et al, 1990.

This idea was also studied by Alcala et al,1995 where they concluded that a solitary wave propagating through the radar volume may provide an explanation for these frequency jumps.

If we compare the model surface with the real power vs space-time plot produced for the 13th of July between 08:00 and 09:00 UT (figure 7.24), we observe how, just where the frequency jump studied at 08:31 UT occurs, PMSE has the same shape as the model shown in figure 7.23, panel A.

Also the relative velocity (Doppler shift) shown in figure 7.23, panel B matches with the real measurements in figure 7.19.

This is not the only reason that makes me think that this frequency jump is probably caused by wave steepening, also the 13th of July between 08:00 and 09:00 UT there are evidences of gravity waves propagating to higher altitudes, for instance just at the same time the frequency jump is observed, the maximum Spectral powers of each gate appear displaced around 17 seconds. This possible signature of gravity wave will be study in section 7.4.

Figure 5.4 shows the spectrogram from 08:00 to 09:00 UT of the 13th of July 2004, and there is noticed more evidences of other possible gravity waves as well as other frequency jumps occurring during this hour. The same events are not observed for the 5th of July where no evidence of gravity waves were found and only the frequency

jump of figure 7.17 is observed. Figure 7.25 shows the power vs space-time plot produced for the 5th of July between 08:00 and 09:00 UT.

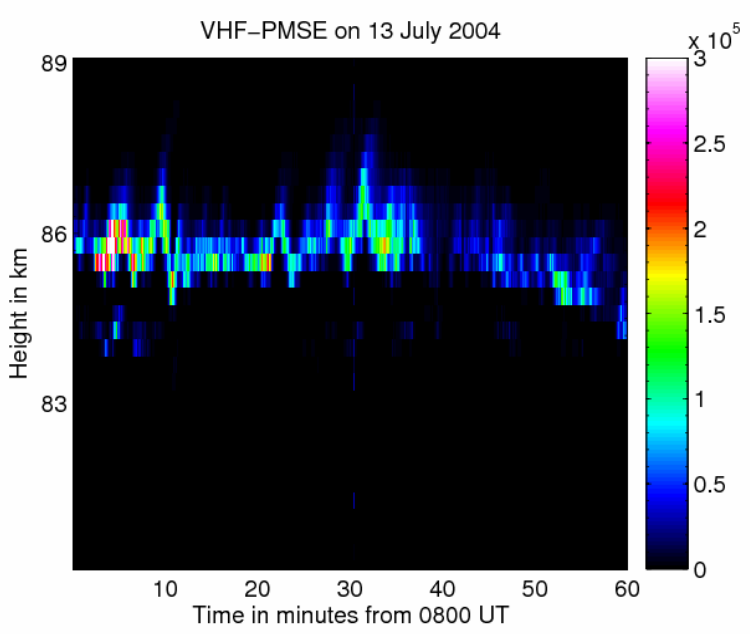

Figure 7.24→ Power vs space-time plot produced for the altitude region 80-89 Km during the PMSE experiment, carried out on 13th July 2004 from 08:00 to 09:00 UT.

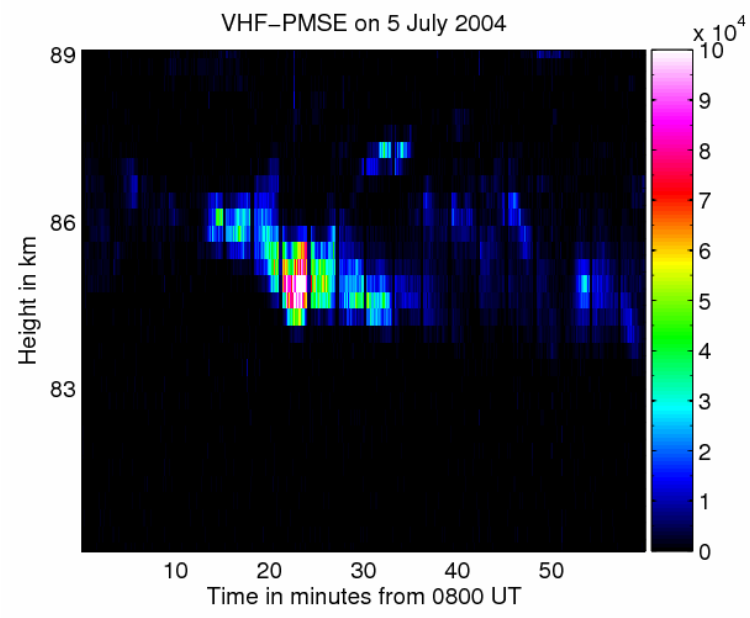

Figure 7.25→ Power vs space-time plot produced for the altitude region 80-89 Km during the PMSE experiment, carried out on 5th July 2004 from 08:00 to 09:00 UT.

7.3.2.2 Breaking wave instability

Another explanation suggested in the past is that a wave breaking into turbulence could cause these frequency jumps (Röttger, J. et al, 1990). The same surface

model with its corresponding Doppler shift as in the wave steepening theory is shown in figure 7.26:

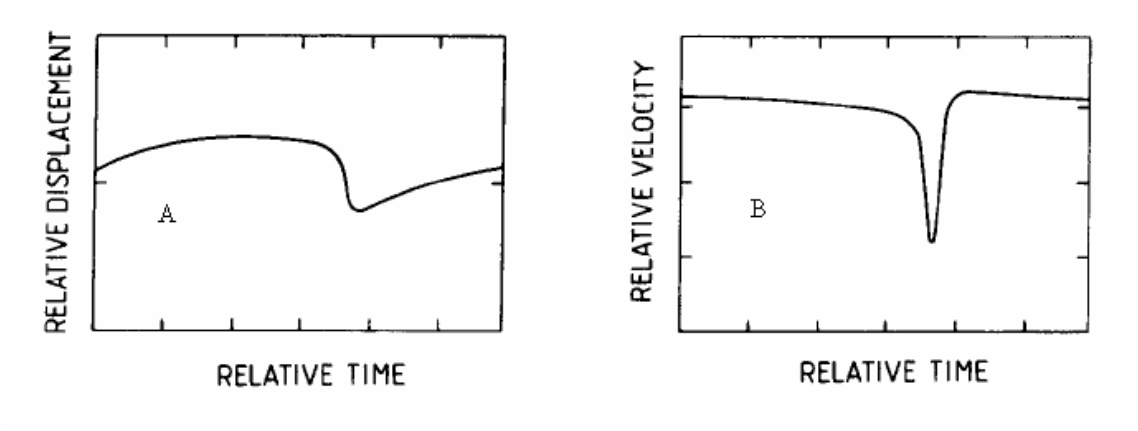

Figure 7.26→ Model surface of a thin layer of turbulence, discontinuity or isentrope in (A) a breaking-wave instability. The corresponding relative velocity (Doppler shift), is shown in panel B. The scales are in arbitrary units. From Röttger, J. et al, 1990.

In our experiment, the power vs space-time plots produced for the 5th (figure 7.25) and the 13th (figure 7.24) of July do not show a PMSE displacement like in figure 7.26, panel A. Also in case a breaking wave occurs, we should see an increase in the echo amplitude which, by looking to our spectral plots, we do not observe.

7.3.2.3 Vortex

Other possibility suggested as possible cause of the frequency jump is that, under the most favourable circumstances, a large vortex would move through the beam causing a fast Doppler velocity reversal (Röttger, J. et al, 1990). The idea of this vortex is explained in diagram 7.2:

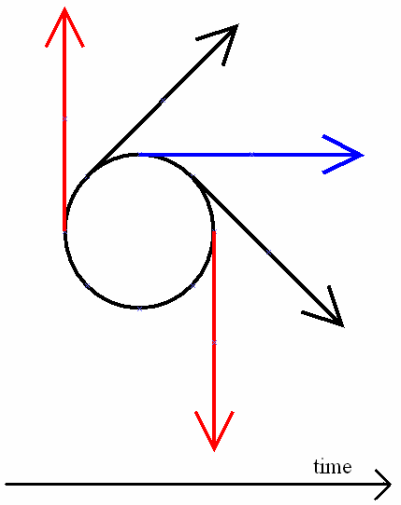

Diagram 7.2→ The diagram represent a Doppler velocity reversal with a negative sign as it could be the one in figure 7.16. The arrows represent the Doppler velocity, in red it means that all the Doppler velocity is in the vertical component (the radar only can measure vertical component) and in blue it means that the vertical component is 0 (the radar would not measure any Doppler velocity)

In the diagram we observe that, in case this theory explains the frequency jumps, we should see echoes with Doppler velocities around 0 for a significant period of time

between the Doppler velocity reversal (in the diagram would be the vertical component of the black vectors).

Considering the vortex model and the new spectral event observed in figure 7.22, in a frequency jump which follows diagram 7.2, the only way both red arrows (the maximum and minimum vertical components) could be observed at the same time is in case that the frequency jump occurs in less than 2 seconds (our maximum time resolution) where, we also should observe Doppler velocities between these two values (the vertical component of the black vectors). The fastest frequency jump we observed is the one of figure 7.16 which occurs in 8 seconds so, it could not be possible to observe at the same time during 6 seconds Doppler velocities of 25 m/s (the maximum) and -25 m/s (the minimum) and Doppler velocities between these two values should be observed. Thus, thanks to the resolution of the frequency jump, we can not support in our measurements a theory for frequency jumps based on the vortex model.

7.3.2.4 Thin PMSE layers

The last possibility suggested in this work is that the frequency jumps could not be real frequency jumps and they could be different Doppler velocities of different PMSE layers, which are very thin and separated in altitude by less than the altitude resolution used in the experiments (300 meters in our case). Thus, if it is the reason, we can not distinguish them and, maybe in future experiments, with a higher altitude resolution this event will be solved.

7.4 GRAVITY WAVES SIGNATURES ON PMSE

Since the first observation of PMSE, a wave structure has been noticed. Therefore lots of studies have been carried out to analyze a possible connection between PMSE and gravity waves, which could be responsible for this special structure. (Röttger et al..,1988), (La Hoz et al., 1989), (Williams et al., 1989), (Röttger et al..,1990), (Hoppe and D.C. Fritts, 1995).

The first objective of my work with the processed data from 2004 EISCAT campaign in Tromsø, was to identify evidences of PMSE layers modulated by gravity waves. Unfortunately, not many clear examples were found, and with a progression in the different layers of PMSE that causes us to doubt whether or not it is a real signature of gravity wave.

In the general observations of chapter 6, some of these possible signatures were reported. In the next figures, we will study two of them, which have been observed the 13th of July between 08:00 and 09:00 UT (Figure 5.4) and some of their basic parameters will be calculated.

In Figure 7.27, between 08:31 and 08:33 UT approximately and from 86.7 Km to 88.8 Km altitude, the PMSE signal seems to be modulated by a gravity wave (the black line in the figure shows the possible constant phase wave front), with an upward

phase propagation which means downward propagation of the wave. This possible signature of a gravity wave appears just above the frequency jump and at the same time, which make us think in the frequency jump as a consequence of wave steepening.

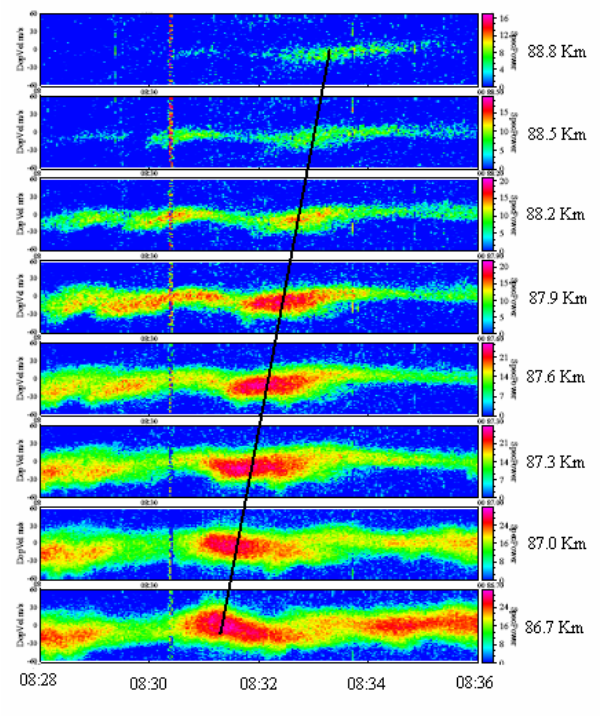

Figure 7.27→ Spectrogram produced for 8 gates with altitudes between 86.7 and 88.8 km altitude during the PMSE experiment, carried out on 13th July 2004 from 08:28 to 08:36 UT. Around 08:31 UT some evidences of PMSE modulated by a gravity wave due to PMSE progression through the different gates . In the altitudes below this spectrogram we observe the frequency jump studied in section 7.3

By looking at the spectrogram we can observe how the maximum spectral power value of the different gates appears displaced in time. In the lowest gate, 86.7 Km altitude, the maximum spectral power value during this interval of time is at 08:31:24 UT and in the highest gate, 88.8 Km, the maximum is at 08:33:44 UT.

With the equation 4.3 we can calculate the vertical phase velocity of the gravity wave, "c_{pz}" (by assuming that the phase wave front is constant) and the vertical wave number, "m_z". The frequency of the wave,"ω", is defined as the Brunt–Väisäla frequency, "ω_B" which is:

Equation 7.1

$$\omega_B = \sqrt{\frac{g}{T}\left(\frac{dT}{dz} + \frac{g}{c_p}\right)}$$

T= temperature g= gravity acceleration

c_p = specific heat of air at constant pressure

Using a typical value of $\omega_B = 10^{-2} s^{-1}$, we can calculate both parameters mentioned above:

From equation 4.3 $$c_{pz} = \frac{dz}{dt} \approx \frac{(88.8 - 86.7)10^3}{(08:33:44) - (08:31:24)} = 15 \text{ m/s}$$

$$m_z = \frac{\omega_B}{c_{pz}} \approx 6.667 \times 10^{-4} m^{-1} \approx \frac{2\pi}{9.424} \frac{1}{Km}$$

And from equation 4.4 we can know the wavelength of the gravity wave:

$$\lambda_z = \frac{2\pi}{m_z} = 9.424 \text{ Km}$$

Figure 7.28 shows another possible signature of gravity wave also from the 13th of July at the same altitudes but, observed 14 minutes before. The black line in the figure shows the possible constant phase wave front, with an upward propagation.

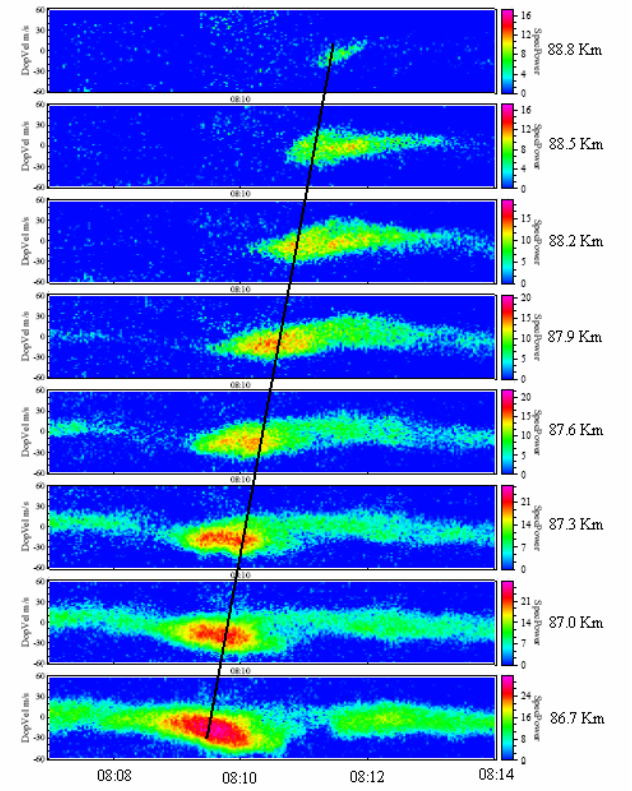

Figure 7.28→ Spectrogram produced for 8 gates with altitudes between 86.7 and 88.8 km altitude during the PMSE experiment, carried out on 13th July 2004 from 08:08 to 08:14 UT. Around 08:31 UT some evidences of PMSE modulated by a gravity wave due to PMSE progression through the different gates . The lowest gate of this plot and the altitudes below it show a frequency jump which can be observed in figure 5.4

By following the same steps than in the other case, the exact time where the maximum PMSE power is received at 86.7 Km is 08:09:38 UT, and at 88.8 Km is 08:11:26 UT. Thus the vertical phase velocity, "c_{pz}", the vertical wave number, "m_z" and the wavelength of the gravity wave are:

$$c_{pz} = \frac{dz}{dt} \approx \frac{(88.8 - 86.7)10^3}{(08:11:26) - (08:09:38)} = 19.44 \text{ m/s}$$

$$m_z = \frac{\omega_B}{c_{pz}} \approx 5.144 \times 10^{-4}\, m^{-1} \approx \frac{2\pi}{12.215} \ \frac{1}{Km}$$

$$\lambda_z = \frac{2\pi}{m_z} = 12.215 \ Km$$

The parameters obtained for this gravity wave are very similar to the others before. Also the values agree with other observations of atmospheric gravity waves with vertical wave numbers around $m_z = \frac{\omega_B}{c_{pz}} \approx \frac{2\pi}{10} \ \frac{1}{Km}$ at 80 Km approximately (Lintelman, S. A. at al, 1994) so, it is possible that the PMSE layer from the 13th of July was modulated by gravity waves.

7.5 CONCLUSIONS

We have shown in detail measurements of PMSE under the influence of two HF heating periods, obtained with EISCAT VHF radar, during the EISCAT campaign 2004 in Tromsø. In the next sections, we will show the conclusions extracted from these studies.

7.5.1 Heating cycles

7.5.1.1 Overshoot effect

With the heating cycle of 20 seconds on and 160 seconds off, examples that follow the Havnes prediction for the behaviour of PMSE power (Havnes et al., 2003) were shown, where, thanks to a time resolution of 2 seconds, it was very clear how the PMSE power decreases during the on periods and how it increases again when the heater is turned off (figure 7.3).

7.5.1.2 Overshoot effect using short cycles of on and off

An attempt to study how large PMSE power can increase with the heating was done by using a different heating cycle with short periods of on and off. This experiment did not contribute to obtain new information about PMSE due to two reasons. The most important was that the chosen period of time for that experiment was not the appropriate one since PMSE had a natural tendency to decrease steadily in time (figure 7.7). The other reason was a different event which has been observed before and which is an absorption of electrons that occurs during the heating process.

7.5.1.3 Correlation between spectral width of PMSE and the heating cycles

In the observation of spectrograms Power vs Doppler velocity-time, a narrowing in the spectral width of PMSE was observed during the heating periods, but a detailed analysis of the spectral width values during these periods concluded that the narrowing

observed was an artefact of the logarithmic scale used to produce the plots. Other tests to try to find a correlation also gave negative results. This conclusion agrees with the idea explained in the theory (section 3.5.3) which says that the heating only affects the electrons while neutral air and ions remain unaffected, as their turbulent motions.

7.5.2 Frequency jumps

In the study of the frequency jumps, a new characteristic of the PMSE spectra during the frequency jump was found when we resolved how the Doppler velocity reversal occurs. The gradual death (decreasing in amplitude) of one Doppler velocity "layer" is observed while a new one appears increasing in amplitude until the frequency jump finishes, where the first Doppler has completely disappeared and the new one has a value equivalent to the one before with opposite sign (figures 7.21 and 7.22). The high time resolution of these experiments has allowed for the first time to resolve in detail how the transition (jump) takes place.

In the cases observed, the abruptness jump found occurs the 13th of July where a discontinuity of the vertical velocity around 56 m/s takes place in less than 10 seconds.

In the attempt to find a model which fits with our observation of frequency jumps, we do not have a conclusive result. Here a list of the results of these analyses to explain the frequency jumps of the 5th and the 13th of July follows:

-The possibility of a model based in a vortex is ruled out in all our measurements due to the incompatibility with the appearance of two spectral peaks (with the maximum and the minimum value) at the same time and the gradual transformation from one to the other.

- A breaking wave instability does not seem to be an option since the expected shape of the PMSE layers during this event is not observed in our measurements. Also other effects of a wave breaking in the atmosphere as an increase in the spectral power are not observed either.

- Wave steepening could explain the frequency jumps of the 13th of July. The expected signature of a gravity wave at these altitudes which increases in amplitude is observed in figure 7.24 just when the frequency jumps occur. Also the expected relative velocity matches with our measurements. However, by looking at the spectrograms Power vs Doppler velocity-time, it is difficult to assure that it is a gravity wave since the spectral amplitude progression through the PMSE layers is not always clear. We calculated different parameters of the possible gravity waves and the results, if not conclusive, they increase the probability of being real signatures of gravity waves propagating through the atmosphere with vertical phase velocities around $c_{pz} \approx 15\text{m/s}$ and vertical wave numbers around $m_z \approx \frac{2\pi}{10}\ \text{Km}^{-1}$

-The last possibility mentioned could explain the frequency jumps observed the 13th of July but, with the same arguments, we can not say the same for the frequency jump observed the 5th of July so, we believe that other sources could be responsible for this type of event like for instance the thin PMSE layers explained in section 7.3.2.4, or maybe others which still are unknown.

7.5.3 Gravity waves

In the analysis of more than 40 hours of PMSE measurements, we did not find many clear examples of possible signatures of gravity waves. The best candidates were found on the 13th of July, especially between 08:00 and 09:00 UT, but these possible gravity waves also showed characteristics which cause us some doubts, like changes in the vertical phase velocity in short periods of time or an inconstant amplitude progression through the PMSE layers. Two of these possible signatures from the 13th of July were analysed because they were the clearest examples and also because of the fact that they appear just above the frequency jumps. The parameters obtained are:

- For the gravity wave observed around 08:11:00 UT: vertical phase velocity $c_{pz} \approx 19.44$ m/s, vertical wave number, $m_z \approx \frac{2\pi}{12.215} \mathrm{Km}^{-1}$ and wavelength $\lambda_z = 12.215$ Km.

- For the gravity wave observed around 08:31:00 UT: vertical phase velocity $c_{pz} \approx 15$ m/s, vertical wave number, $m_z \approx \frac{2\pi}{9.424} \mathrm{Km}^{-1}$ and wavelength $\lambda_z = 9.424$ Km.

These values seem to be possible values of atmospherical gravity waves so we think that, at least during this day, PMSE might be modulated by gravity waves.

REFERENCES

- Alcala, C. M., Rötger, J. and Kelley, M.C.: Spatial interferometry measurements of polar mesosphere summer echoes with the EISCAT VHF radar. Radio Science, 30(4):1205-1218 (1995)

-Balsley, B. B. and Huaman, M.: On the relationship between seasonal occurrence of northern hemispheric polar mesosphere summer echoes and mean mesopause temperatures, J. Geophys. Res.,102, 2021–2024 (1997).

Balsley, B. B., Ecklund, W. L., and Fritts, D. C.: VHF echoes form the high-latitude mesosphere and lower thermosphere: observations and interpretations, J. Atmos. Sci., 40, 2451–2466 (1983).

- Belova, E., P. B. Chilson, M. Rapp, and S. Kirkwood: Electron temperature dependence of PMSE power, Adv. Space. Res., 28, 1077–1082 (2001).

-Belova, E., Chilson, P., Kirkwood, B., S. and Rietveld M. T.: The response time to ionospheric heating. Journal of geophysical research, VOL. 108, NO. D8, 8446, doi:10.1029/2002JD002385 (2003).

-Chilson, P., Belova, E., Kirkwood, B., S., Rietveld M. T. and Hoppe, U.P.: First artificially induced modulation of PMSE using the EISCAT heating facility. Geophysical research letters, 27(23):3801-3804 (2000).

-Cho, J.Y.N., and Rötger, J.: An updated revier of Polar mesospheric summer echoes: Observation, theory, and their relatioship to noctilucent clouds and subvisible aerosols. Journal of geophysical research, VOL. 102, NO. D2, 2001-2020 (1997).

-Czechowsky, P., Reid, I.M. and Rüster, R.: VHF radar measurements of the aspect sensitivity of the summer polar mesopause echoes over Andenes (69ºN, 16ºE), Norway. Geophysical research letters, 15(11): 1259-1262 (1988).

-Ecklund, W. L. and Basley B.B.: Long term observations of the Artic mesosphere with the MST radar at Poker Flat, Alaska. Journal of geophysical research, 86(A9): 7775-7780 (1981)

-Fritts, D.C., and Alexander, M.J.: Gravity wave dynamics and effects in the middle atmosphere. Rev. Geophys., 41(1), 1003, doi:10.1029/2001RG000106 (2003).

-Gumbel, J., Siskind, D. E., Witt, G., Torkar, K. M., and Friedrich M.: Influences of ice particles on the ion chemistry of the polar summer mesosphere. Journal of geophysical research, VOL. 108, NO. D8, 8436, doi:10.1029/2002JD002413 (2003).

-Hagfors, T.: Note on the scattering of electromagnetic waves from charged dust particles in a plasma. J. Atmos. Terr. Phys.., 54, 333-338 (1992).

-Havnes, O., Alasken, T. and Brattli, A.: Charged Dust in the Earth´s Middle Atmosphere. Physica Scripta. Vol. T89, 133-137 (2001).

-Havnes, O.: Polar mesospheric summer echoes (PMSE) overshoot effect due to cycling of artificial electron heating. Journal of geophysical research, VOL. 109, A02309, doi:10.1029/2003JA010159 (2004).

-Havnes, O., La Hoz, C., and Næsheim, L. I.: First observations of the PMSE overshoot effect and its use for investigating the conditions in the summer mesosphere. Geophysical research letters, VOL. 30, NO. 23, 2229, doi:10.1029/2003GL018429 (2003).

Hoppe, U.P., Hall, C. and Rötger, J.: First observation of summer polar mesosphere backscatter with 224 MHz radar. Geophysical research letters, 15(1):28-31 (1988).

-La Hoz, C.: Radar scattering from dusty plasmas. Phys. Scr., 45, 529-534 (1992).

-La Hoz, C., O. Havnes, L.I. Naesheim and D.L. Hysell, JGR: Observations and theories of Polar Mesospheric Summer Echoes at a Bragg wavelength of 16 cm,.Vol 111, D04203 (2006).

- La Hoz, C., L. I. Næsheim, O. Havnes, and M. T. Rietveld : First observation of the artificial electron heating induced reduction of the PMSE strength at 933 MHz. Manuscript, EISCAT Workshop (2003).

-Lintelman, Scott A., and Gardner Chester S.:Observation and interpretation of spectra of atmospheric gravity waves perturbations with upward and downward phase progression. Journal of geophysical research, VOL 99, NO.D8, 16959-16971 (1994).

-Rapp, M., and Lübkeb F.-J.: Polar mesosphere summer echoes(PMSE): review of observations and current understanding. Atmospheric Chemistry and Physics 4, 2601-2633 (2004).

- Reid, I.M., Czechowsky, P., Rüster, R. and Schmidt G.: First VHF radar measurements of mesopause summer echoes at mid-latitudes. Geophysical research letters, 16(2):135-138 (1989).

- Rapp, M., and F.-J. Lübkeb: Electron temperature control of PMSE, Geophysical research letters., 27, 3285– 3288 (2000).

-Röttger, J., La Hoz, C., Franke, S., J., Liu, C.H.: Steepening of reflectivity structures detected in high-resolution Doppler spectra of polar mesosphere summer echoes (PMSE) observed with the EISCAT 224 MHz radar. Journal of Atmopheric and Terrestrial Physics Vol. 52, No IO/I I, pp. 939-954 (1990).

-Röttger, J., La Hoz, C.: Characteristics of polar mesosphere summer echoes (PMSE) observed with the EISCAT 224 MHz radar and possible explanations of

their origin. Journal of Atmopheric and Terrestrial Physics, VOL. 52, NO. 10/11, 893-906 (1990).

- Röttger, J., La Hoz, C., Kelley, M.C., Hoppe, U.P. and Hall, C.: The structure and dynamics of polar mesospher summer echoes observed with the EISCAT 224 MHz radar. Geophysical research letters, 15(12):1353-1356 (1988)

-Scales, Wayne: Electron temperature effects on small-scale plasma irregularities associated with charged dust in the earth's mesosphere.

-Tian-You Yua, Palmer, R. D. and Chilson P.B.: An investigation of scattering mechanisms and dynamics in PMSE using coherent radar imaging. Journal of Atmospheric and Solar-Terrestrial Physics 63 1797–1810 (2001).